

2/83

CMCRCZ 12 (2), 61-116 (1983)

ΧΗΜΙΚΑ ΧΡΟΝΙΚΑ

ΝΕΑ ΣΕΙΡΑ

CHIMIKA CHRONIKA

NEW SERIES

**AN INTERNATIONAL EDITION
OF THE GREEK CHEMISTS ASSOCIATION**

MANAGING COMMITTEE

Irene DILARIS, Yannis GAGLIAS, Vassilios M. KAPOULAS, Vassilios LAMBROPOULOS,
Georgia MARGOMENOU - LEONIDOPOULOU, Panayotis PROUNTZOS, George SKALOS

Ex-officio Members: Panayotis PAPADOPOULOS (Asst. Gen. Secretary of G.C.A.),
Stelios CHATZIYANNAKOS (Treasurer of G.C.A.).

EDITORS - IN - CHIEF

V.M. KAPOULAS G. SKALOS G. MARGOMENOU - LEONIDOPOULOU

EDITORIAL ADVISORY BOARD

N. ALEXANDROU

Org. Chem., Univ. Salonica

A. ANAGNOSTOPOULOS

Inorg. Chem., Tech. Univ. Salonica

D. BOSKOS

Org. Chem., Tech., Univ. Salonica

P. CATSOULACOS

Pharm. Chem., Univ. Patras

G.D. COUMOULOS

Physical Chemistry Athens

C.A. DEMOPOULOS

Biochemistry, Univ. Athens

C.E. EFSTATHIOU

Anal. Chem., Univ. Athens

A.E. EVANGELOPOULOS

Biochemistry, N.H.R.F., Athens

S. FILIANOS

Pharmacognosy, Univ. Athens

D.S. GALANOS

Food Chem., Univ. Athens

A.G. GALINOS

Inorg. Chem., Univ. Patras

P. GEORGAKOPOULOS

Pharm. Techn., Univ. Salonica

I. GEORGATSOS

Biochemistry, Univ. Salonica

M.P. GEORGIADIS

Org./Med. Chem., Agr. Univ. Athens

N. HADJICHRISTIDIS

Polymer Chem., Univ. Athens

T.P. HADJIIOANNOU

Anal. Chem., Univ. Athens

E. HADJOUDIS

Photochem., N.R.C. «D», Athens

D. JANNAKOUDAKIS

Phys. Chem., Univ. Salonica

N.K. KALFOGLOU

Polymer Sci., Univ. Patras

E. KAMPOURIS

Polymer Chem., Tech. Univ. Athens

M.I. KARAYANNIS

Anal. Chem., Univ. Ioannina

N. KATSANOS

Phys. Chem., Univ. Patras

A. KEHAYOGLOU

Org. Chem. Tech., Univ. Salonica

D. KIOUSSIS

Petrochemistry, Univ. Athens

A. KOSMATOS

Org. Chem., Univ. Ioannina

P. KOUROUNAKIS

Pharm. Chem., Univ. Salonica

S.B. LITSAS

Bioorg. Chem., Arch. Museum, Athens

G. MANOUSSAKIS

Inorg. Chem., Univ. Salonica

I. MARANGOSIS

Chem. Mech., Tech. Univ. Athens

I. NIKOKAVOURAS

Photochem., N.R.C. «D», Athens

D.N. NICOLAIDES

Org. Chem., Univ. Salonica

C.M. PALEOS

N.R.C. «Democritos», Athens

V. PAPADOPOULOS

N.R.C. «Democritos» Athens

G. PAPAGEORGIOU

Biophysics, N.R.C. «D», Athens

V.P. PAPAGEORGIOU

Nat. Products, Tech. Univ. Salonica

S. PARASKEVAS

Org. Chem., Univ. Athens

G. PHOKAS

Pharmacognosy, Univ. Salonica

S. PHILIPAKIS

N.R.C. «Democritos», Athens

G. PNEUMATIKAKIS

Inorg. Chem., Univ. Athens

C.N. POLYDOROPOULOS

Phys/Quantum Chem., Univ. Ioannina

K. SANDRIS

Organic Chem., Tech. Univ. Athens

M.J. SCOULLOS

Env./Mar. Chem., Univ. Athens

C.E. SEKERIS

Mol. Biology, N.H.R.F., Athens

G.A. STALIDIS

Phys. Chem., Univ. Salonica

Ch. STASSINOPOULOU

N.R.C. «Democritos», Athens

A. STASSINOPOULOS

Argo AEBE Athens

A. STAVROPOULOS

Ind. Technol., G.S.I.S., Piraeus

I.M. TSANGARIS

Inorg. Chem., Univ. Ioannina

G. TSATSARONIS

Food Technol., Univ. Salonica

G.A. TSATSAS

Pharm. Chem., Univ. Athens

A.K. TSOLIS

Chem. Technol., Univ. Patras

G. VALCANAS

Org. Chem., Tech. Univ. Athens

A.G. VARVOGLIS

Org. Chem., Univ. Salonica

G.S. VASSILIKIOTIS

Anal. Chem., Univ. Salonica

S. VOLIOTIS

Instrum. Analysis, Univ. Patras

E.K. VOUDOURIS

Food Chem., Univ. Ioannina

I. VOURVIDOU - FOTAKI

Org. Chem., Univ. Athens

I.V. YANNAS

Mech. Eng., M.T.I., U.S.A.

Correspondence, submission of papers, subscriptions, renewals and changes of address should be sent to Chimika Chronika, New Series, 27 Kaningos street, Athens, Greece. The Guide to Authors is published in the first issue of each volume, or sent by request. Subscriptions are taken by volume at 500 drachmas for members and 1.000 drachmas for non-members in Greece and 28 U.S. dollars to all other countries except Cyprus, where subscriptions are made on a cash basis.

Printed in Greece by ATHANASOPOULOS-PAPADAMIS-ZACHAROPOULOS, G.P.

76, EMM. BENAKI ATHENS (145)

Υπεύθυνος σύνταξης με το νόμο: Παναγιώτης Ευθάλης, Κάνιγγος 27, Αθήνα (147).

CONTENTS

Comparative bioavailability studies of four commercial nitrofurantoin products (in English) <i>by P.E. Macheras</i>	63
Polarographic and thermodynamic study of the complex ion $\text{Pb}(\text{OH})_3^-$ in aqueous-methanol, aqueous-acetonitrile and aqueous-dioxane solutions (in English) <i>by D.Jannakoudakis and N. Missaelidis</i>	75
Concentration and storage of peroxyacetylnitrate (PAN) for mobile field measurements in tropospheric air (in English) <i>by S. Glavas and U. Schurath</i>	89
Synthesis under pressure of a new series of rare earth perovskites with formula $\text{TCu}_{3-x}\text{Mn}_{4+x}\text{O}_{12}$ (in French) <i>by D. Samaras</i>	99
Sport paper	
A simple method for the determination of gas permeability values of various films used in food and drug packaging applications (in English) <i>by M.G. Kontominas, E. Hatzidimitriou and E.K. Voudouris</i>	111

COMPARATIVE BIOAVAILABILITY STUDIES OF FOUR COMMERCIAL NITROFURANTOIN PRODUCTS

PANAYOTIS E. MACHERAS

Laboratory of Pharmaceutical Chemistry, Athens University, 104 Solonos street, Athens (144), Greece.

(Received September 23, 1982)

Summary

The relative bioavailability of nitrofurantoin in four commercial products marketed in Greece was examined in 4 subjects using a Latin square design. The urinary excretion method was used and the data obtained were analysed according to a one-compartment open model. Analysis of variance was performed on all parameters calculated. Statistically significant differences were found between the products examined. Dissolution tests were performed and *in vitro* - *in vivo* correlations were developed. These findings prove that the tested products can not be utilized interchangeably.

Key words : Bioequivalence, *in vitro* - *in vivo* correlation, analysis of variance.

Introduction

It is well known that the compliance of commercially available products with the compendial requirements does not necessarily imply their bioequivalence¹⁻⁵. This problem is most acute in Greece where a list similar to that of Food and Drug Administration⁶ for the drugs requiring bioavailability testing has not been issued. Consequently, bioequivalence regulations are not applied and relevant studies have not been reported. It was therefore of primary importance to perform a bioequivalence study for products marketed in Greece to provide the indispensable information for appropriate prescription.

Nitrofurantoin was chosen as a model drug since it exhibits bioavailability problems^{7,8} and a total of 46 dosage forms (27 companies) are commercially available on the Greek market. Four formulations (3 tablets, 1 capsule) were examined and dissolution tests were undertaken to establish any correlation of *in vitro* - *in vivo* data.

Materials and Methods

Nitrofurantoin products were obtained directly from the manufacturers prior to

December, 1981. Specifications of the formulations are given in Table I. Analysis of 6 tablets or capsules of each brand detected no significant difference in nitrofurantoin content.

Dissolution test

The rotating basket method was used for the dissolution studies. One tablet or capsule was placed into a 250 mesh screen basket and the whole was immersed in 1 lit. beaker containing 400 ml of the dissolution medium (HCl 0.1 N or phosphate buffer pH 7.2). The basket was rotated at 60 rpm at 3 cm distance from the bottom of the beaker. The whole assembly was maintained at 37° in a constant temperature bath. Samples of 5 ml were collected at 5,10,20,30,40,50,60, and 70 min. Five milliliters of dissolution medium maintained at 37° was added to the beaker after each sample was removed. Each 5 ml sample was filtered (millipore 0.45 µm) and 1.0 ml aliquot was diluted to 10.0 ml with purified water. Absorbance was read at 380 nm against a blank of the corresponding diluted dissolution medium.

Bioavailability study

Two male and two female volunteers took part in the study. Their ages ranged from 28 to 35 years with a weight range 49-70 kg. Each subject gave a written informed consent. The volunteers were instructed to refrain from taking any other drug a week before and during the trials. Each subject ingested a 100 mg tablet or capsule of a nitrofurantoin product every 72 hr in accordance with the assigned schedule (Table I).

TABLE I: Latin square design for the evaluation of nitrofurantoin bioavailability.

Subject	Day			
	1	4	7	10
1	A	B	C	D
2	D	C	A	B
3	C	D	B	A
4	B	A	D	C

Key: A = Funit, tablets lot 81010, Ladrug Laboratories, Athens. B = Furonitran tablets, lot 14, Defarm Laboratories, Athens. C = Macroclantin capsules (nitrofurantoin in macrocrystals), lot 105. D = Furadantin tablets lot 103. Brands C and D are prepared in Greece by N. Petsiavas A.E. under the supervision of Morton Norwich Products Inc.

Because the bioavailability of nitrofurantoin is greater when taken with food⁹ but many patients have a tendency not to take their medications as prescribed by the physician, the dose was administered in the morning 1 h after a light breakfast

of 150 ml milk and 50 g of bread. Since the urinary excretion method has been suggested¹⁰ as the preferred method for the determination of nitrofurantoin bioavailability, urine samples were collected at 0,1,2,3,4,6,8,12,24 h, ensuring each time complete emptying of the bladder. In order to stimulate urine output, 150 ml of water were ingested after each urine collection. All samples were frozen to ensure stability of drug and convenience of analysis. The samples were allowed to thaw immediately before use. The amounts of drug in urine were determined according to the method of Conklin and Hollifield¹¹ as modified by Mendes et al¹².

Results and Discussion

Dissolution studies. The results of the dissolution tests are presented in Fig 1 and 2. For the plotting a correction factor¹³ was taken into account. At both pH used the products A and B showed remarkably higher dissolution profiles to those obtained from C and D. The rapid dissolution of the products A and B was in accordance with their fast disintegration¹⁴ (< 1 min) in 0.1 N HCl in comparison to the 7.5 min. found for D. As far as the product C is concerned the low dissolution rate was expected since the drug is in macrocrystalline form. The change of the

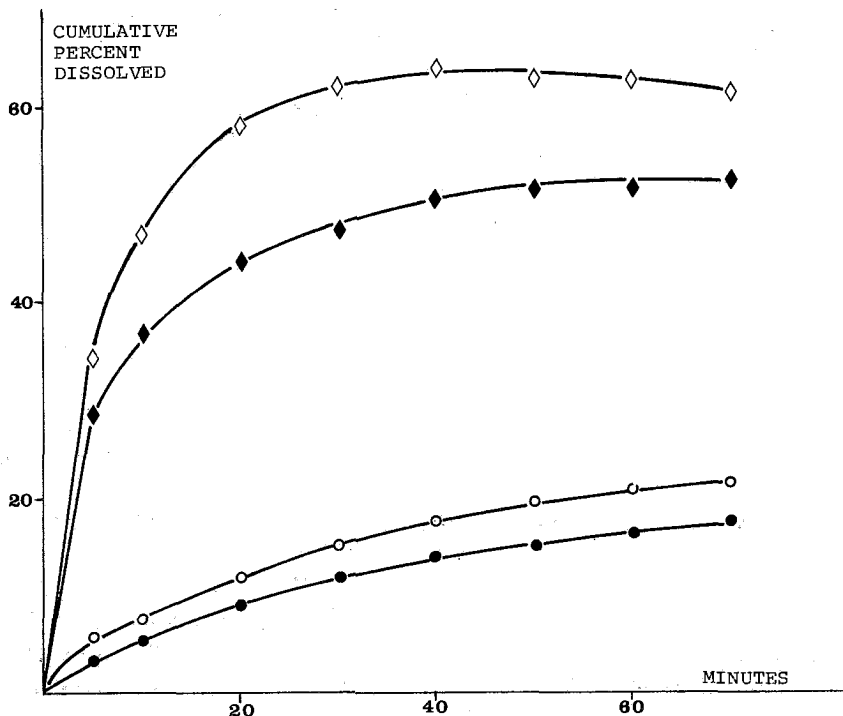


FIG. 1 : Dissolution profiles for nitrofurantoin at pH 1.0. Each data point is the mean of three determinations. Key : \diamond brand A, \blacklozenge brand B, \circ brand C, \bullet brand D.

dissolution profile for brands C and D depicted in Fig 1 and 2 is probably attributed to formulation factors.

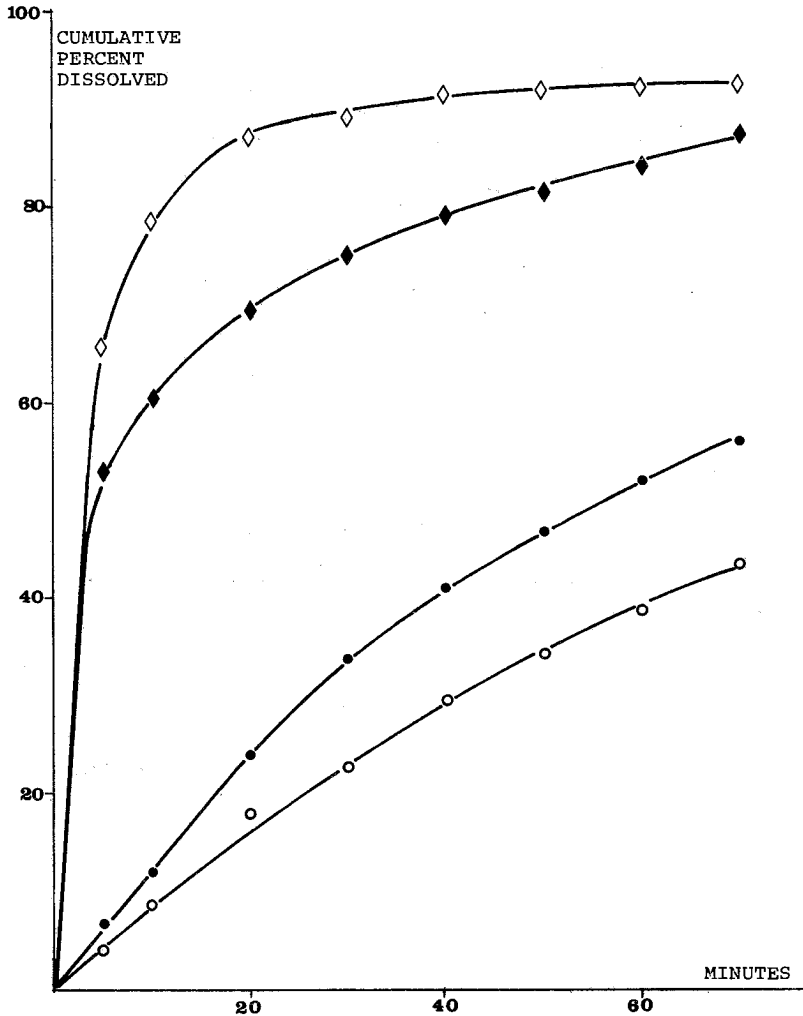


FIG. 2 : Dissolution profiles for nitrofurantoin at pH 7.2. Each data point is the mean of three determinations. Key : see Fig. 1.

Bioequivalency. Since no appreciable amount of drug was found in the 24 h specimen for all treatments and subjects the total amount excreted in urine over 12 h was proved sufficient to describe the extent of nitrofurantoin bioavailability. Figure 3 presents the cumulative amount of nitrofurantoin recovered as unchanged drug in urine versus time. It can be seen that the product C has a lower bioavailability than the other formulations. In parallel, Fig 4 shows the mean

excretion rate profile of the formulations. Product C is the only exhibiting a sort of sustained release action.

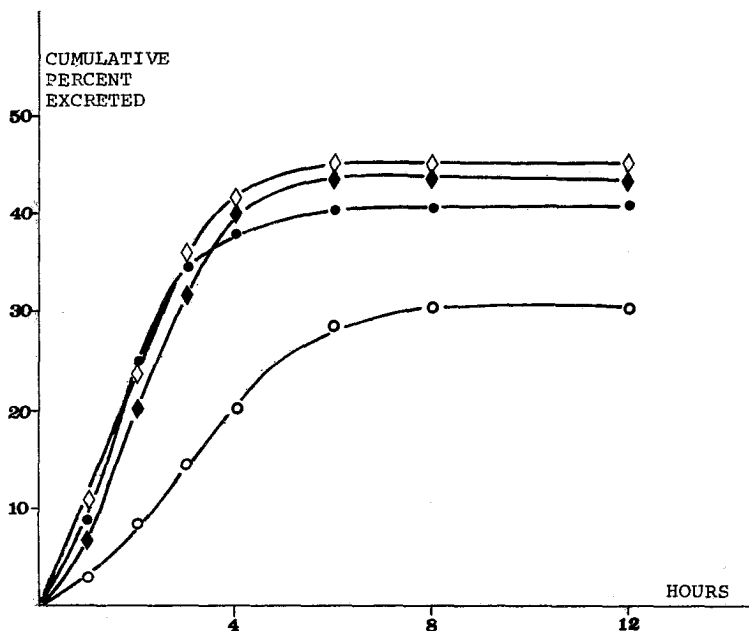


FIG. 3 : Mean cumulative percent of nitrofurantoin excreted versus time. Each data point is the mean cumulative percent excreted for all four subjects. Key : see Fig. 1.

The experimental results obtained were further analyzed according to a one-compartment open model using the equation (2) which is valid instead of the known relationship¹⁵ (1) for the special case $k = k_a$ (see Appendix),

$$X_t = F \left[1 - \frac{1}{k_a - k} (k_a e^{-kt} - k e^{-k_a t}) \right] \quad (1)$$

$$X_t = F [1 - (1 + Kt) e^{-Kt}] \quad (2)$$

where X_t is the percent of drug excreted in time t , F is the percentage of total drug excreted, k_a is the absorption rate constant, k is the elimination rate constant, and K is the common value of the two rate constants e.g. $k = k_a = K$. The use of the simpler equation (2) was made for two reasons. Firstly, nitrofurantoin exhibits rapid absorption and excretion while the elimination half life is essentially independent of the dosage form¹⁰. In addition, the results quoted by Mendes et al¹² and the excretion rate profile given by Mattok et al⁷ indicate the validity of approximation $k = k_a$. Secondly, equation (1) involves three parameters F , k , k_a not identifiable using the method of non-linear least squares. Admittedly each

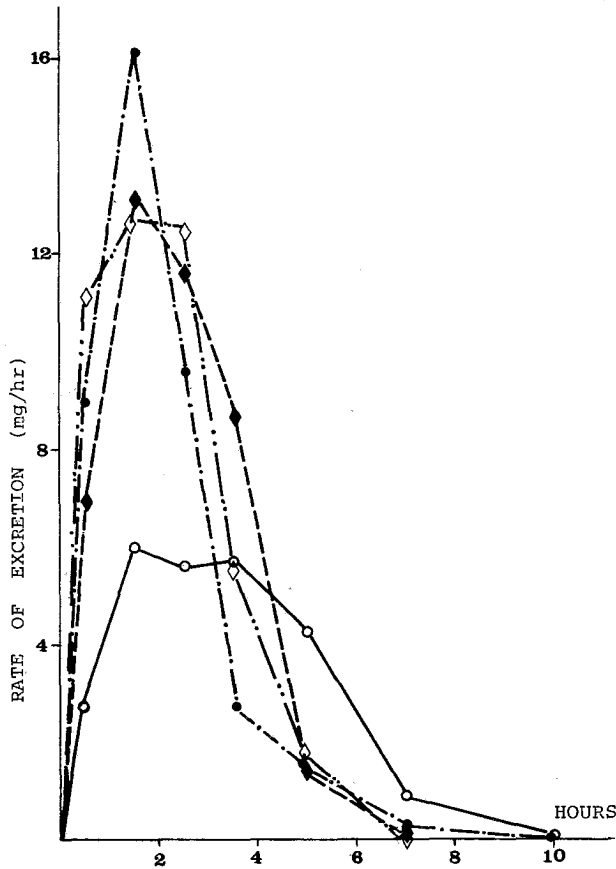


FIG. 4 : Mean excretion profiles of nitrofurantoin products. Key : see Fig. 1.

parameter can be separately calculated from the experimental data, namely, F from the cumulative amount excreted (Fig. 3) while k or k_a by standard graphing procedures. However, each calculation is accomplished with an accuracy involving a standard error s_F , s_k , s_{k_a} for each parameter. If one of the three parameters, say F , is chosen and imposed on the model, it follows that s_F will be transferred to the other two parameters. Therefore, to avoid biased estimation of the parameters the approximation quoted was used as a better simulation of the *in vivo* process.

The experimental data were subjected to computer non-linear least square method of analysis using the program NONLIN¹⁶ to obtain the best estimates for the model described by equation (2). The values obtained for F and K as well as for the peak excretion time t_{max} (eq.3) and the peak excretion rate Q (eq. 4)

$$t_{max} = \frac{1}{K} \quad (3), \quad Q = \frac{D.F.K}{e} \quad (4)$$

where D represents the dose, are given in Table II.

TABLE II : Values of the parameters of nitrofurantoin formulations.

Formulation	F ^a , %	K ^a , hr ⁻¹	t _{max} ^a , hr	Q ^a , mg/hr
A	47.05(4.94)	1.10(0.56)	1.12(0.57)	18.62(8.81)
B	44.98(5.65)	0.94(0.42)	1.19(0.41)	14.99(4.72)
C	32.24(6.92)	0.54(0.11)	1.90(0.40)	6.45(1.80)
D	41.61(4.06)	1.07(0.31)	1.02(0.40)	16.09(3.87)

a : Mean values of four subjects with standard deviation in parentheses.

Analysis of variance was performed on the four parameters estimated and the results obtained are summarized in Table III. The tabulation of variance reveals that the formulations are different in terms of F, t_{max} and Q. Also, the subject variability seems to be significant for t_{max} while no period effect was observed.

TABLE III : Analysis of variance (ANOVA). Critical Fisher's f for 3 and 9 degrees of freedom at p:0.05 is 3.86.

Source of variation	Variance - f test			
	F	K	t _{max}	Q
Formulations (3) ^a	171.6 (7.187)	0.263(2.689)	0.635(5.354)	111.8 (4.775)
Subjects (3) ^a	49.15(2.059)	0.307(3.145)	0.461(3.885)	48.87(2.087)
Residual (9) ^a	23.87	0.098	0.119	23.42

a : Degrees of freedom.

Since significant f ratios were detected a further analysis of variance was applied comparing all possible couples of formulations. Significant difference (p = 0.05) in drug parameters calculated for the brands studied was found, Table IV. Brand C was significantly different from D for all parameters calculated, and from A for the parameters F and t_{max}. In addition brands A and D were significantly different in terms of F. The differences for the parameter F observed between the pairs of brands C-D and A-C could be attributed either to formulation factors or to a different extent of food influence on the bioavailability of drug. However, the dissolution profiles depicted in Fig. 1 and 2 indicate that the differences between brands A and C as well as between A and D, most likely arise from formulation factors. It has been proved⁹ that food enhances the bioavailability of nitrofurantoin more intensively when ingested in macrocrystalline than in microcrystalline form. Since similar dissolution profiles were found for brands C and D (Fig. 1 and 2), a

TABLE IV. Significant differences in drug parameters for the brands studied.

Parameter	Brands					
	A and B	A and C	A and D	B and C	B and D	C and D
F	N.S	*	*	N.S	N.S	*
K	N.S	N.S	N.S	N.S	N.S	*
t_{max}	N.S	*	N.S	N.S	N.S	*
Q	N.S	N.S	N.S	N.S	N.S	*

Key : * = significant at 0.05 level, N.S = not significant at 0.05 level.

study was undertaken coadministering brands C or D with breakfast to find out if bioavailability of brand C can be attributed to the 1h non-compliance interval. The bioavailability design was the standard, two period crossover for four subjects and two formulations. All other conditions and methods were identical with those described above. Examination of the results obtained for period, intra- and inter-subject variability did not reveal any statistically significant difference. The experimentally calculated mean cumulative percent of drug excreted for brands C and D was 33.87% and 44.10% respectively. These values show a similar increase,

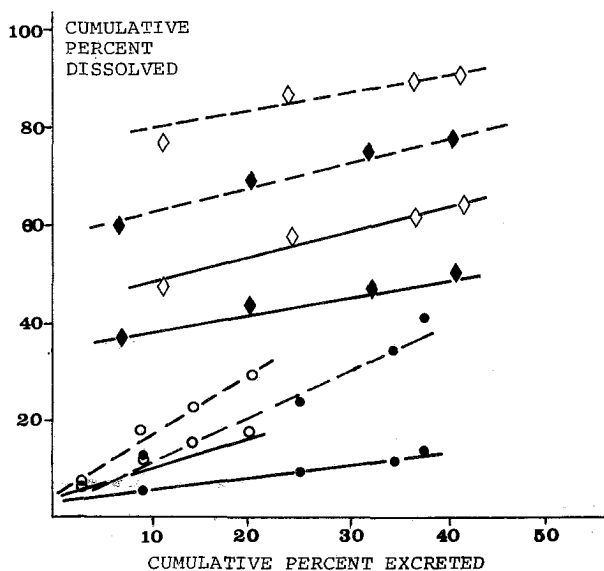


FIG. 5 : Correlation of mean cumulative of nitrofurantoin excreted in 1.0, 2.0, 3.0 and 4.0 h following the oral administration of nitrofurantoin brands with mean cumulative percent dissolved in 10, 20, 30 and 40 min in pH 7.2 (---) or pH 1.0 (—). Key : see Fig. 1.

namely 5% and 6% respectively when compared with the corresponding values given in Table II. It is concluded therefore that bioavailability differences between brands C and D are caused by formulation factors and not from variations in drug food interaction. Accordingly, the dissolution test did not ideally reflect the rate of drug absorption. Thus, product D appears to have been made available much more rapidly for absorption than product C (Fig. 3) but this could not have been predicted from the *in vitro* test, (Fig. 1,2).

Nevertheless, the multiple point *in vitro-in vivo* correlation depicted in Fig. 5 was excellent ($R > 0.95$) for all brands. It should be noted however, that the intercepts on the *in vitro* axis for brands A and B are 76% and 57% respectively at pH 7.2 while for C and D are near zero. Since intensity factors or lag time corrections were not employed and *in vitro* test conditions were identical for all brands studied, the high intercepts on the abscissa for brands A and B are not due to improper agitation. It is quite apparent therefore that the rapid release of drug from brands A and B is attributable to formulation factors.

An overall correlation for the percentage of total drug excreted versus the cumulative drug dissolved at 1h, resulted in a correlation coefficient of 0.90 (Fig. 6). This value can be considered as reasonable in terms of the small number of brands utilized and their diversity in manufacturing procedures.

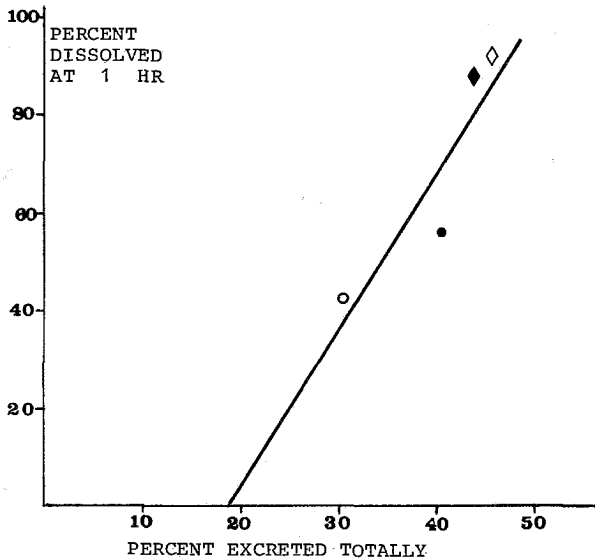


FIG. 6 : Correlation of percent excreted totally in urine versus the percent dissolved in pH 7.2 at 1 hr for the four nitrofurantoin brands studied. Key : see Fig. 1.

The results obtained gave a clear view of the remarkable differences between the brands studied. Thus, brands A and B did not meet the dissolution specification for nitrofurantoin of USP XIX: "Between 25% and 60% of the labelled amount in the tablets dissolves at one hour". Though, USP XX simply states that not less than

25% of the drug dissolves in 60 minutes. In the light of the official recommendations, the reformulation of brands A and B is advisable. Moreover, brand C just passed the *in vitro* test (Fig. 2) which was reflected in a significantly lower bioavailability than brands A and D (Table IV). Brand D is in accordance with the *in vitro* test criteria even though the dissolution tests (Fig. 1 and 2) anticipated for a lower bioavailability. The latter was found to be 41.61%, quite similar to 41.48% reported previously¹² for the same product marketed in USA. However, the analysis of variance (Table IV) proved that brands C and D can not be used interchangeably. The same is apparently applied to the pairs of brands A and C as well as A and D (Table IV).

Appendix

The amount of intact drug in plasma (as percentage of the total drug) X_p under the conditions of $k = k_a = K$ is described¹⁷ as:

$$X_p = FKte^{-Kt}$$

while the urinary excretion rate is given by the equation:

$$\frac{dX}{dt} = KX_p = K^2 Fte^{-Kt}$$

The last equation can be integrated for $t=0$, $X=0$ and $t=t$, $X=X_t$ to yield,

$$X_t = K^2 F \left[-e^{-Kt} \frac{(Kt + 1)}{K^2} \right]_0^t \quad \text{or} \quad X_t = F [1 - (1 + Kt)e^{-Kt}]$$

Περίληψη

Συγκριτική μελέτη της βιοδιαθεσιμότητας τεσσάρων σκευασμάτων Νιτροφουραντοΐνης.

Η Νιτροφουραντοΐνη είναι ένα από τα φάρμακα που παρουσιάζει κυμαινόμενη βιοδιαθεσιμότητα μεταξύ χημικά ισοδυνάμων σκευασμάτων. Στη μελέτη αυτή προσδιορίστηκε με τη μέθοδο της ουρικής απέκκρισης η βιοδιαθεσιμότητα τεσσάρων σκευασμάτων νιτροφουραντοΐνης που κυκλοφορούν στην Ελληνική αγορά. Τα πειραματικά δεδομένα αναλύθηκαν με τη μέθοδο των μη γραμμικών ελαχίστων τετραγώνων βασισμένη σε ένα απλοποιημένο μονοδιαμερισματικό μοντέλο. Οι παράμετροι που υπολογίστηκαν, υποβλήθηκαν σε ανάλυση της ποικιλίας (ANOVA) αποκαλύπτοντας την βιο-ανισοδυναμία (bio-inequivalence) για τρία ζεύγη σκευασμάτων.

Συσχετισμοί *in vitro* - *in vivo* έδωσαν υψηλούς συντελεστές συμμεταβολής.

References and Notes

1. Arnold K. and Gerber N.: *Clin. Pharmacol. Ther.* **11**, 121 (1970).
2. McGilveray I.J., Mattok G.L., and Hossie R.D.: *J. Pharm. Pharmacol.* **23**, 246 S (1971).
3. McGilveray I.J., Mattok G.L., and Hossie R.D.: *Rev. Can. Biol.* **32**, 99 (1973).
4. Wagner J.G., Christensen M., Sakmar E., Blair D., Yate J.D., Willis P.W., Sedman A.J. and Stoll R.J.: *J. Am. Med. Assoc.* **224**, 199 (1973).
5. Meyer M.C., Slywka G.W.A., Dann R.E. and Wyatt P.L.: *J. Pharm.Sci.*, **63**, 1693 (1974).
6. Fed. Regist. **40**, 26164 (1975).
7. Mattok G.L., Hossie R.D., and McGilveray I.J.: *Can. J. Pharm. Sci.* **7**, 84 (1972).
8. DiSanto E.R., Chodos D.J., Philips J.P., DeSante K.A., and Stoll R.G.: *Int.J.Clin. Pharmacol.* **13**, 220 (1976).
9. Bates T.R., Sequeira J.A., and Tembo A.V.: *Clin. Pharmacol. Therap.* **16**, 63 (1974).
10. Conklin J.D.: *Antib. Chemother.* **25**, 233 (1978).
11. Conklin J.D. and Hollifield R.D.: *Clin.Chem.* **11**, 925 (1965).
12. Mendes R.W., Masih S.Z. and Kanumuri R.R.: *J.Pharm. Sci.* **67**, 1616 (1978).
13. Malinowski H.J. and Smith W.E.: *J. Pharm. Sci* **63**, 285 (1974).
14. Disintegration times were determined using an apparatus conforming to the USP XIX page 650.
15. Ritshell W.A.: *Handbook of Basic pharmacokinetics Drug intelligence Publications*, Hamilton (1976).
16. Metzler C.M. NONLIN A computer program for parameter estimation in nonlinear situations. The Upjohn Co, Kalamazoo, Michigan (1969).
17. Niazi S.: *Textbook of Biopharmaceutics and Pharmacokinetics*. Appleton-Century Crofts, New York (1979).

Acknowledgements

For the fitting of the experimental data by means of the computer program the author is grateful to Dr A. Iliadis.

POLAROGRAPHIC AND THERMODYNAMIC STUDY OF THE COMPLEX ION $Pb(OH)_3^-$ IN AQUEOUS-METHANOL, AQUEOUS-ACETONITRILE AND AQUEOUS-DIOXANE SOLUTIONS

D. JANNAKOUDAKIS AND N. MISSAELIDIS

Laboratory of Physical Chemistry of the Faculty of Physics and Mathematics, University of Thessaloniki

(Received October 8, 1982)

Summary

The polarographic and thermodynamic behaviour of the complex ion $Pb(OH)_3^-$ in aqueous-methanol, aqueous-acetonitrile and aqueous-dioxane solvents — for different concentrations of the organic solvent — is studied.

The dissociation constant (K) and the coordination number (p) values of the complex are, in each case, calculated by means of the half wave potential values shift. It is proved that the variation of pK against the % v/v concentration of the organic solvent is influenced by the chemical factor (solvation phenomena) as well as by the physical factor (dielectric constant of the medium). These two factors in the case of H_2O-CH_3OH and H_2O-CH_3CN solvent systems act competitively; at low concentrations of the organic solvent the influence of the chemical factor predominates and so there is a decrease of the complex stability, while at higher concentrations the influence of the chemical factor vanishes and only the influence of the physical factor remains effective, thus causing an increase of the complex stability with increasing organic solvent % v/v concentration. For the latter, the complex pK is linearly dependent upon the reverse dielectric constant of the medium.

In the case of aqueous-dioxane solutions, due to the non perceptible change in the extent of solvation with the addition of dioxane, the influence of the physical factor is retained even at low concentrations of dioxane.

Key words: Polarography, complex ion $Pb(OH)_3^-$, stability constant, aqueous-organic solvents.

Introduction

It is well known that the study of complex metallic ions with the polarographic technique is based on the fact that the half wave potential of the depolarizer reduction in the presence of the ligand, $(E_{1/2})_{\text{compl.}}$, is shifted to more negative values compared to that in the absence of the ligand, vis $(E_{1/2})_{\text{free}}^1$.

From these shifts and from the concentrations of ligand we can calculate the formation (stability) constant or the dissociation (instability) constant and the coordination number (p), i.e. the composition of the complex²⁻⁴.

These calculations are valid only when the oxidation or reduction process of the complex on the dropping mercury electrode (D.M.E.) proceeds reversibly³⁻⁷. In this case the following equation is valid:

$$\Delta E_{1/2} = (E_{1/2})_{\text{compl}} - (E_{1/2})_{\text{free}} = \frac{0,0591}{n} \log K - p \cdot \frac{0,0591}{n} \log [L] \quad (1)$$

The equation (1) represents a straight line according to the formula:

$$y = a + bx, \text{ where } y = \Delta E_{1/2}, x = \log [L],$$

$$a = \frac{0,0591}{n} \log K \quad \text{and} \quad b = -p \cdot \frac{0,0591}{n}$$

Thus from the diagram of the $\Delta E_{1/2}$ values against logarithm of the ligand concentration $[L]$ (since the electron number value, n , is known) it is possible to calculate both the dissociation constant, K , and the coordination number, p , of the corresponding complex.

The equation (1) is valid supposing that the diffusion coefficient of the complex ions is similar to that of the free ions. If this is not true, then the corresponding diffusion coefficients should also be introduced in the equation (1); so the equation (1) takes the following form:

$$\Delta E_{1/2} = \frac{0,0591}{n} \log K \sqrt{\frac{D_{\text{compl.}}}{D_{\text{free}}}} - p \cdot \frac{0,0591}{n} \log [L] \quad (2)$$

The ratio $\sqrt{\frac{D_{\text{compl.}}}{D_{\text{free}}}}$ is easily calculated because it is equal to $\frac{(i_d)_{\text{compl.}}}{(i_d)_{\text{free}}}$,

provided that the solvent system, the temperature and the capillary characteristics are the same and also the complex and free ions concentrations are equal.

However, if the depolarizer reduction takes place irreversibly, in order to use equation (1), we should previously calculate the values $(E_{1/2})_{\text{compl.}}$ and $(E_{1/2})_{\text{free}}$ corresponding to a reversible reaction. This is possible as far as the part of the polarographic wave corresponding to the commencement of the electroreduction can be considered as reversible regardless of the fact that the overall reduction is an irreversible one. This part of the polarogram corresponds to the reduction of the depolarizer ions which are in the interfacial region of the D.M.E., before the diffusion from the bulk starts⁸.

Thus after the logarithmic analysis of the irreversible polarogram (i.e. plotting the E values against $\log \frac{i}{i_d - i}$) by extrapolating the straight line which corre-

sponds to the reversible part of the wave, we can find $E_{1/2}^{\text{rev}}$ value from the cut of the extrapolated straight line with the zero current line (fig. 1).

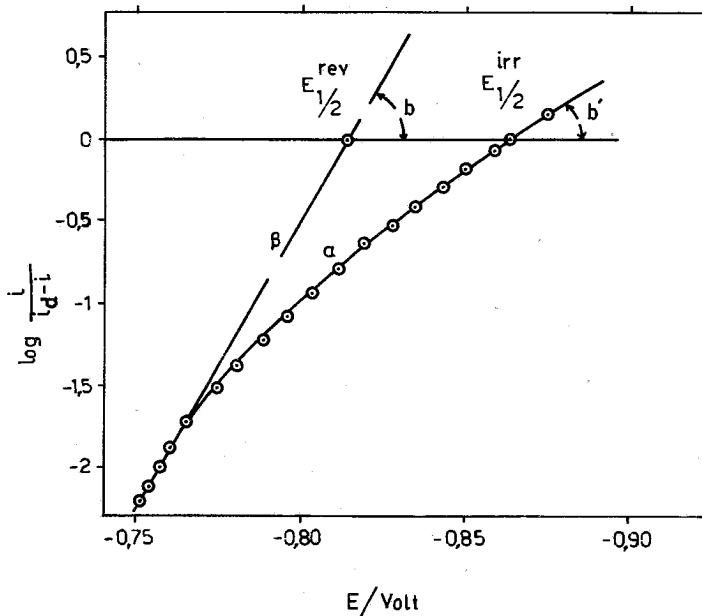


FIG. 1 : Logarithmic analysis of a polarogram with $[\text{Pb}^{++}] = 10^{-3} \text{ M}$ and $[\text{OH}^-] = 0,6 \text{ M}$ in the presence of $0,4 \text{ M KNO}_3$ ($I=1$) in aqueous - isopropanol solution 10 % v/v in isopropanol.


So by calculating in this way the $E_{1/2}^{\text{rev}}$ values for the irreversible waves we can use again equation (1) to find the K and p values.

In the present work we wanted to investigate the polarographic behaviour of the simple complex ion $\text{Pb}(\text{OH})_3^-$ in aqueous-organic solvent systems which are widely used in modern Electrochemistry, such as the aqueous-methanol, aqueous-acetonitrile and aqueous-dioxane solutions, for different concentrations of the organic solvent. The purpose of this study was to determine the influence of the chemical factor, that is the extent of the solvation phenomenon. We also wanted to determine the influence of the physical factor (i.e. the influence of the medium dielectric constant) on the reduction potential and on the thermodynamic stability, or the pK , of this simple complex ion, which is widely used for the electrolytic deposition of lead on various metallic and other electrode surfaces.

Experimental

For the study of the complex $\text{Pb}(\text{OH})_3^-$ in the above mixed solvents a Metrohm Herisau polarograph, type Polarecord E 261 was used. An Ag/AgCl electrode as well as a S.C.E. (saturated calomel electrode) were used as reference electrodes.

The substances and the solvents used in the overall experimental study, with their purity degree and manufacturing company, are presented below:

a)	$\text{Pb}(\text{NO}_3)_2$, rein kristallisiert	, Merck
b)	KNO_3	, reinst (puriss)	, Merck
c)	KOH	, titrisol solution	, Merck
d)	KCl	, reinst (puriss)	, Merck
e)	CH_3OH	, puriss p.a.	, Fluka A.G.
f)	CH_3CN	, puriss p.a.	, Fluka A.G.
g)		, depurato	, Carlo Erba

All the solvents used were of high purity grade (puriss p.a.); on the other hand, where that was necessary (dioxane), a chemical refining process and evaporation under low pressure conditions was carried out (b.p. of dioxane: 101 °C).

During the experimental process the cell with its content as well as the reference electrode were sunk in a thermostatic bath having constant temperature $t = 25 \pm 0,1$ °C (by means of a Haake thermostat).

The solutions used had final ionic strength equal to 1 ($I = 1$), so that even high concentrations of the ligand could be added. So the ligand concentration was always higher (100 to 1000 times) than that of the depolarizer (Pb^{++}), which is necessary to keep the bulk and interfacial concentration practically constant. Evidently the ionic strength of every solution was practically equal to the sum of the ligand and the supporting electrolyte concentrations.

Results and discussion

At the beginning, the polarographic behaviour of the complex $\text{Pb}(\text{OH})_3^-$ was studied in aqueous solutions, in order to compare our results with those of Lingane and Vlček, who also studied this reduction in aqueous solutions⁹⁻¹⁰.

A series of measurements from different solutions with constant depolarizer concentration, $[\text{Pb}(\text{NO}_3)_2] = 10^{-3}$ M, was obtained. Potassium nitrate was used as supporting electrolyte. In order to study the influence of the ligand concentration on the $E_{1/2}$ potential of the depolarizer, increasing quantities of sodium hydroxide were introduced in the solution starting from a system with zero ligand concentration and always keeping the solution ionic strength equal to unit.

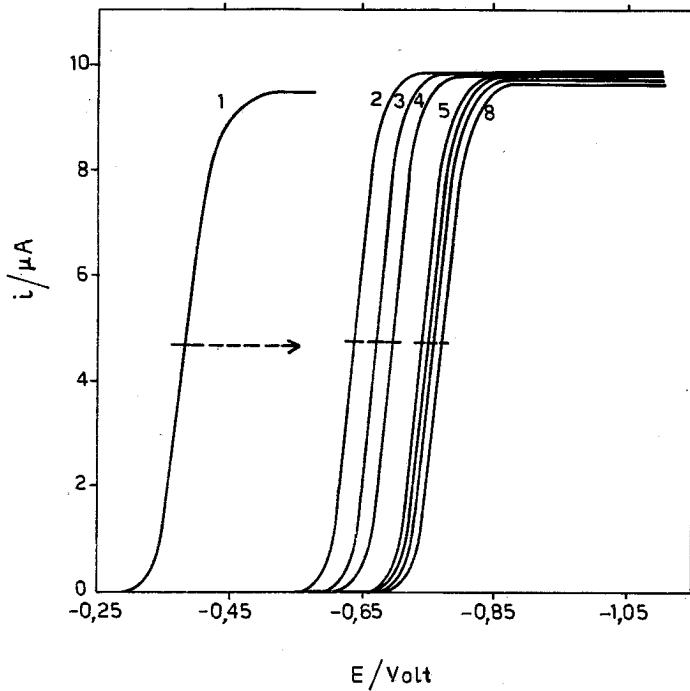
In table I the values of $E_{1/2}$ as well as those of $\Delta E_{1/2}$ corresponding to the ligand concentrations (OH^-) for the different solutions are provided.

In fig. 2 the positions of the polarograms corresponding to the solutions N° 1 to 8 of table I are also provided as an example.

These polarograms are electrochemically reversible, as this is also proved by

TABLE I : $E_{1/2}$ and $\Delta E_{1/2}$ values for the different concentrations of ligand (OH^-) in aqueous solutions. $[Pb^{++}] = 10^{-3}$ M, ref. electrode: Ag/AgCl, $t = 25$ °C.

N°	sup.electrolyte concentration (M)	ligand concentration (M)	$\log C_{OH^-}$	$E_{1/2}$ Volt	$\Delta E_{1/2}$ Volt
1	1	0	—	-0,365	—
2	0,95	0,05	-1,301	-0,634	-0,269
3	0,90	0,10	-1,000	-0,665	-0,300
4	0,80	0,20	-0,699	-0,691	-0,326
5	0,50	0,50	-0,301	-0,730	-0,365
6	0,30	0,70	-0,155	-0,743	-0,378
7	0,20	0,80	-0,097	-0,750	-0,385
8	0	1	0	-0,755	-0,390

FIG. 2 : Shift of $E_{1/2}$ of Pb^{++} with increasing concentration of the ligand (OH^-) in aqueous solutions. C_{OH^-} : 1) 0, 2) 0,05, 3) 0,1, 4) 0,2, 5) 0,5, 6) 0,7, 7) 0,8, 8) 1 M.

their logarithmic analysis. In other words the $\log \frac{i}{i_d - i}$ is always a linear function of the potential E .

The logarithmic analysis of the polarogram N° 2 is shown, as an example, in fig. 3.

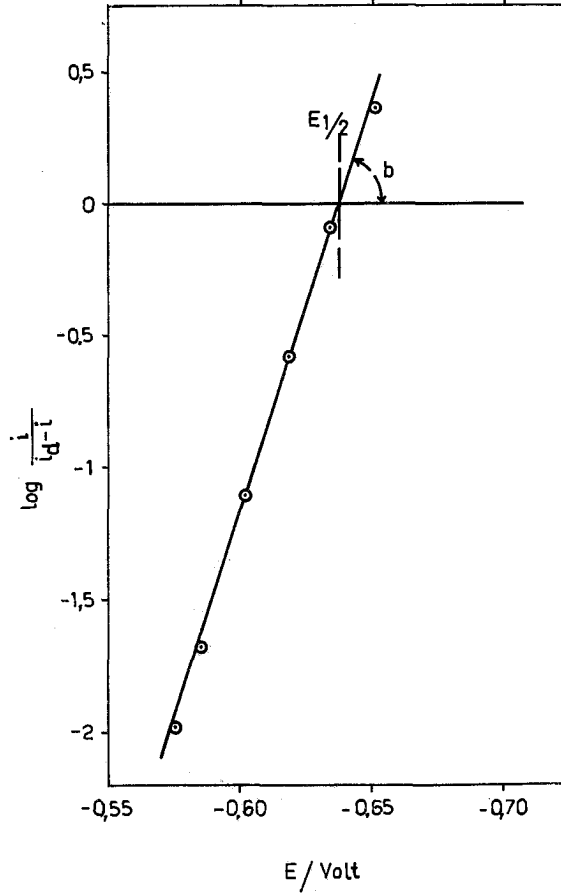
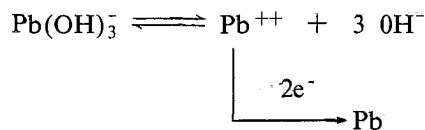


FIG. 3 : Logarithmic analysis of a polarogram with $[Pb^{++}] = 10^{-3} M$ and $[OH^-] = 0,05 M$ in the presence of $0,95 M KNO_3$ ($I = 1$) in aqueous solution.

The slope of the straight line in this diagram is equal to $-\frac{1}{0,029} \text{ Volt}^{-1}$ and it corresponds to an electron number equal to 2.

So the following reaction will take place:



The values of $\Delta E_{1/2}$ plotted against $\log C_{\text{OH}^-}$, fig. 4, give a straight line, as provided by the equation (1).

This straight line has a linear correlation coefficient:

$$r^2=0,999, \quad a=-0,392 \quad \text{and} \quad b=-0,094.$$

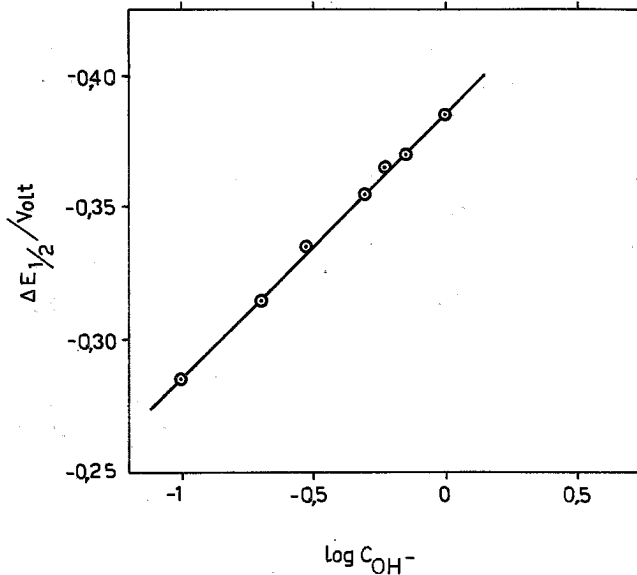


FIG. 4 : Dependence of $\Delta E_{1/2}$ on $\log C_{\text{OH}^-}$ for the values of table I.

This fact proves that the reduction observed on the electrode surface corresponds to that of the free lead ions, which are continuously produced from the complex dissociation.

Therefore by means of the above equation we can calculate the dissociation constant and the coordination number of the complex examined, in aqueous solutions. That is:

$$b = -p \cdot \frac{0,0591}{n} = -0,094 \quad \text{and because } n=2, \text{ then:}$$

$$p = \frac{0,094 \cdot 2}{0,0591} = 3,18 \approx 3.$$

$$\text{On the other hand : } a = \frac{0,0591}{n} \log K = -0,392 \quad \text{or}$$

$$\log K = -\frac{0,392 \cdot 2}{0,0591} = -13,27. \quad \text{So : } K = 5,42 \cdot 10^{-14} \quad \text{and } pK = 13,27.$$

The value $\log K = -13,27$ (for ionic strength equal to 1) is in satisfactory agreement with the value $\log K = -12,8$ calculated by Lingane, as well as with the value $\log K = -13,95$ obtained by extrapolation to zero ionic strength, Vlček¹⁰. On the other hand the coordination number is equal to 3.

In the aqueous-methanol solutions the behaviour of the above complex was studied for the following % v/v concentrations of CH₃OH : 5, 10, 15, 20, 25 and 30.

The study for higher concentrations was not possible because of solubility problems of the depolarizer Pb(NO₃)₂ as well as of the supporting electrolyte (KNO₃).

The logarithmic analysis of all polarograms recorded proved that the polarographic behaviour of the complex Pb(OH)₃⁻ is absolutely reversible for the overall methanol concentrations used, just as it happens in the aqueous solutions.

In table II the values of $E_{1/2}$ and $\Delta E_{1/2}$ as a function of the ligand (OH⁻) concentration for aqueous-methanol solutions 5 % v/v in CH₃OH are provided.

In fig. 5 we show the dependence of $\Delta E_{1/2}$ on $\log C_{OH^-}$ for the values of table II.

TABLE II : $E_{1/2}$ and $\Delta E_{1/2}$ values for the different concentrations of ligand (OH⁻) in aqueous-methanol (5 % v/v CH₃OH) solutions [Pb²⁺] = 10⁻³ M, ref. electrode: Ag/AgCl, t = 25 °C.

N°	sup.electrolyte concentration (M)	ligand concentration (M)	$\log C_{OH^-}$	$E_{1/2}$ Volt	$\Delta E_{1/2}$ Volt
1	1	0	—	-0,325	—
2	0,9	0,1	-1,000	-0,610	-0,285
3	0,8	0,2	-0,699	-0,640	-0,315
4	0,7	0,3	-0,523	-0,660	-0,335
5	0,5	0,5	-0,301	-0,680	-0,355
6	0,4	0,6	-0,222	-0,690	-0,365
7	0,3	0,7	-0,155	-0,695	-0,370
8	0	1	0	-0,710	-0,385

In table III the results of the complex study in aqueous-methanol solutions, that is the K and p values for the different concentrations of CH₃OH are also tabulated.

Finally in fig. 6, using the values of table III, the dependence of the complex pK on the % v/v concentration of CH₃OH in the solution is shown. In the same figure we also provide the dependence of pK on $\Delta (1/\epsilon) = (1/\epsilon_s - 1/\epsilon_w)$, for the various methanol concentrations employed. In the above figure ϵ_s and ϵ_w are the dielectric constants of aqueous-methanol and aqueous solution respectively.

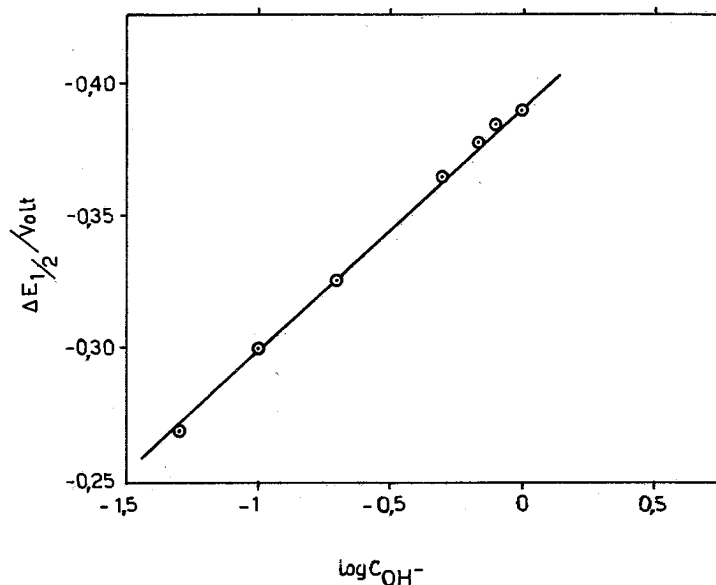


FIG. 5 : Dependence of $\Delta E_{1/2}$ on $\log C_{\text{OH}^-}$ for the values of table II.

TABLE III : Polarographic and thermodynamic data of the complex $\text{Pb}(\text{OH})_3^-$ in aqueous-methanol solutions. $t = 25^\circ \text{C}$.

% v/v	K	pK	ϵ	$\Delta \left(\frac{1}{\epsilon} \right) \cdot 10^4$	n	p
CH ₃ OH						
5	$8.73 \cdot 10^{-14}$	13,06	76,78	3	2	3
10	$2,04 \cdot 10^{-13}$	12,69	74,65	7	2	3
15	$2,58 \cdot 10^{-13}$	12,59	72,53	11	2	3
20	$2,04 \cdot 10^{-13}$	12,69	70,40	15	2	3
25	$1,89 \cdot 10^{-13}$	12,72	68,27	19	2	3
30	$1,28 \cdot 10^{-13}$	12,89	66,15	24	2	3

The polarographic behaviour of the complex $\text{Pb}(\text{OH})_3^-$ was also studied in aqueous-acetonitrile solutions for the following % v/v concentrations of CH₃CN: 2,5 , 5 , 7,5 , 10 , 15 , 20 , 25.

The study for higher concentrations of CH₃CN was not again possible because of solubility problems of the depolarizer as well as of the supporting electrolyte.

The logarithmic analysis of all the polarograms recorded for the different

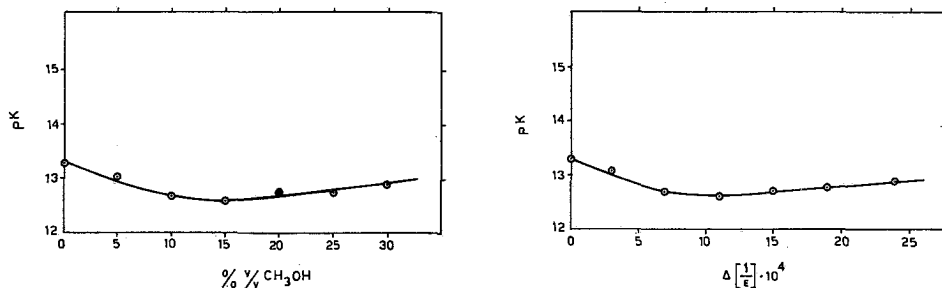


FIG. 6 : Dependence of pK on the % v/v concentration of CH_3OH and on $\Delta(1/\epsilon)$ for the various methanol concentrations.

concentrations of CH_3CN showed that the polarographic behaviour of the complex is reversible up to 15% v/v in CH_3CN , while at higher concentrations it becomes irreversible. Thus, for the concentrations where the polarographic waves are irreversible, we followed the process described at a preceding part of this work for the calculation of $E_{1/2}^{rev}$ value and the slope b (which correspond to a reversible process) in order to calculate the K and p values from equation (1).

In table IV we provide the results of the complex study in aqueous-acetonitrile solutions for the different concentrations of CH_3CN .

TABLE IV : Polarographic and thermodynamic data of the complex $Pb(OH)_3^-$ in aqueous - acetonitrile solutions. $t = 25^\circ C$.

% v/v CH_3CN	K	pK	ϵ	$\Delta\left(\frac{1}{\epsilon}\right) \cdot 10^4$	n	p
2,5	$9,36 \cdot 10^{-14}$	13,03	77,70	1,4	2	3
5	$1,62 \cdot 10^{-13}$	12,79	76,55	3	2	3
7,5	$2,21 \cdot 10^{-13}$	12,66	76,16	4	2	3
10	$1,28 \cdot 10^{-13}$	12,89	74,25	7,4	2	3
15	$8,66 \cdot 10^{-14}$	13,06	73,46	9	2	3
20	$3,97 \cdot 10^{-14}$	13,40	71,67	12	2	3
25	$1,23 \cdot 10^{-14}$	13,91	69,88	16	2	3

Using the values of the table IV, in figure 7 the dependence of the complex pK upon the solution CH_3CN concentration as well as upon the $\Delta(1/\epsilon)$ values for the different concentrations of CH_3CN is shown.

The polarographic behaviour of the complex $Pb(OH)_3^-$ was finally studied in aqueous-dioxane solutions for the following % v/v concentrations of dioxane: 5, 10, 15, 20, 25.

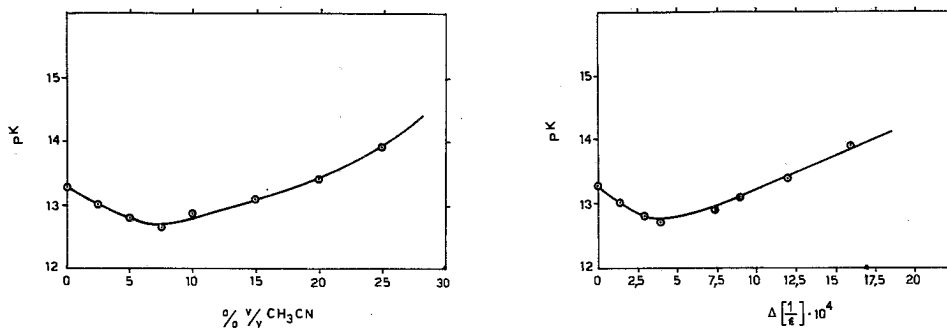


FIG. 7 : Dependence of pK on the % v/v concentration of CH_3CN and on $\Delta(1/\epsilon)$ for the various acetoniile concentrations.

Because of the same reason (solubility problem of the depolarizer and the supporting electrolyte) the study for higher concentrations of dioxane was not possible.

The logarithmic analysis of all the polarograms recorded for the five concentrations of dioxane shows that in this case the polarographic reduction of the complex takes place quite irreversibly. So following the above process the $E_{1/2}^{\text{rev}}$ value and the slope b of the reversible part were calculated for all the waves, before the use of equation (1) for the calculation of the complex K and p values.

In table V the results of the complex study in aqueous-dioxane solutions for the different concentrations of dioxane are given.

TABLE V : Polarographic and thermodynamic data of the complex $\text{Pb}(\text{OH})_3^-$ in aqueous-dioxane solutions. $t = 25^\circ\text{C}$.

% v/v dioxane	K	pK	ϵ	$\Delta\left(\frac{1}{\epsilon}\right) \cdot 10^4$	n	p
5	$2,13 \cdot 10^{-14}$	13,67	74,49	7	2	3
10	$4,48 \cdot 10^{-15}$	14,35	70,25	15	2	3
15	$3,70 \cdot 10^{-16}$	15,43	65,98	24	2	3
20	$3,87 \cdot 10^{-17}$	16,41	61,73	35	2	3
25	$2,73 \cdot 10^{-18}$	17,56	57,47	47	2	3

Using the values of table V in fig. 8 the dependence of the complex pK upon the solution dioxane concentration as well as upon the $\Delta(1/\epsilon)$ values for the different concentrations of dioxane is shown.

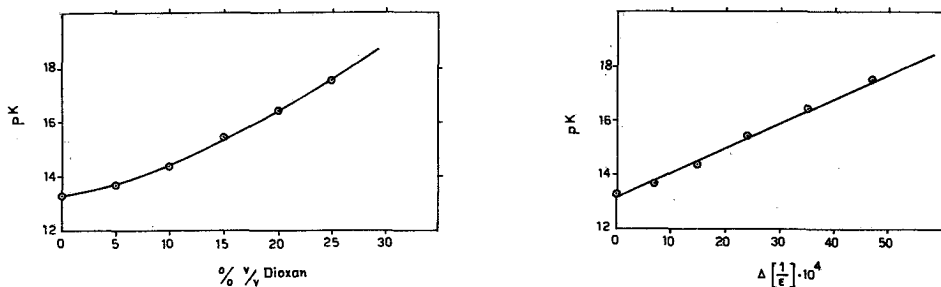


FIG. 8 : Dependence of pK on the % v/v concentration of dioxane and on $\Delta(1/\epsilon)$ for the various dioxane concentrations.

After the overall experimental study of the polarographic behaviour of the complex $Pb(OH)_3^-$ in mixed, with different organic solvents, aqueous solutions we come to the following general conclusions:

In the case of aqueous-methanol and aqueous-acetonitrile solutions (for the latter only up to 15 % v/v concentration) the addition of the organic solvent does not cause any change to the thermodynamic reversibility of the electroreduction, while in the case of aqueous - dioxane solutions it causes a remarkable change of the electrode reaction from electrochemically reversible to an irreversible one.

Generally the introduction of the organic solvent into the solution causes a change to the complex thermodynamic stability. This change of the complex thermodynamic stability with increasing concentration of the organic solvent in the solution is influenced both by the chemical factor (change of the solvation extent) as well as by the physical factor (change of the medium dielectric constant). These two factors in the case of aqueous-methanol and aqueous-acetonitrile solutions, with a relatively low concentration of the organic solvent, act competitively. So, in the case of the mixed solvent systems $H_2O - CH_3OH$ and $H_2O - CH_3CN$, at low concentrations of the organic solvent, the influence of the chemical factor predominates and there is a decrease of the complex stability, while at higher concentrations the influence of the chemical factor vanishes and only that of the physical factor remains effective thus causing an increase to the complex stability with increasing organic solvent % v/v concentration. On the other hand the pK dependence upon $\Delta(1/\epsilon)$ is satisfactorily linear, just as the Born equation generally foresees for the ionisation of electrolytic substances in mixed aqueous-organic solvents with different dielectric constant values¹¹⁻¹⁵.

In the case of aqueous-dioxane solutions, because of the non perceptible change of the solvation extent, there is no influence of the chemical factor and so the pK change with increasing dioxane concentration is exclusively influenced by the physical factor and it is linearly dependent on $\Delta(1/\epsilon)$ for the overall concentrations range studied.

Thus, in general, we can say that the influence of the chemical factor — where it appears — on the complex pK takes place always at low concentrations of the organic solvent, while at higher concentrations the influence of the physical factor predominates.

In fig. 9 we show the thermodynamic stability of the complex ion $Pb(OH)_3^-$ in the different solvent systems studied.

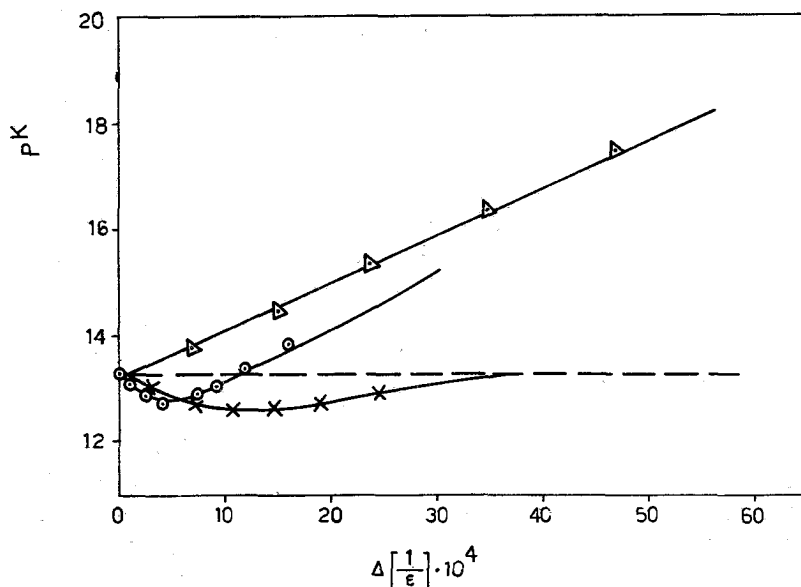


FIG. 9 : Dependence of the complex pK on $\Delta(1/\epsilon)$ for the various concentrations of the organic solvent in the various mixed solvent systems studied (--- aqueous, $\odot \odot \odot$ aqueous-acetonitrile, $\times \times \times$ aqueous-methanol $\Delta \Delta \Delta$ aqueous-dioxane solutions)

The experimental study has proved that the complex $Pb(OH)_3^-$ is in the aqueous-dioxane solutions thermodynamically more stable than in the other mixed solutions. It should be emphasized that in the aqueous-dioxane solutions the reduction potential of the complex shifts to very negative values.

On the other hand, in the aqueous-methanol solutions the thermodynamic stability of the complex is almost the same with that of the aqueous solutions; that is, the pK values are about similar to that of the aqueous solutions.

Finally it must be mentioned that, at the point where the influence of the chemical factor vanishes and that of the physical factor emerges, the product $i_d \sqrt{\eta}$ (η : viscosity coefficient) is constant in all cases studied. This fact means that the radius of the depolarizer ionic components remains constant¹⁶.

Περίληψη

Πολαρογραφική και θερμοδυναμική μελέτη του συμπλόκου ιόντος $Pb(OH)_3^-$ σε υδατομεθανολικά, υδατοακετονιτριλικά και υδατοδιοξανικά διαλύματα.

Μελετάται η πολαρογραφική και θερμοδυναμική συμπεριφορά του συμπλόκου ιόντος $Pb(OH)_3^-$ σε υδατομεθανολικά, υδατοακετονιτριλικά και υδατοδιοξανικά διαλυτικά συστήματα για διάφορες περιεκτικότητες σε οργανικό διαλύτη.

Υπολογίζονται για κάθε περίπτωση βάσει των μετατοπίσεων των τιμών του δυναμικού μισού κύματος, η τιμή της σταθεράς διαστάσεως του συμπλόκου (K) και του αριθμού συναρμογής (p) αυτού. Διαπιστώνεται ότι η μεταβολή του pK συναρτήσεται της % v/v περιεκτικότητας σε οργανικό διαλύτη επηρεάζεται τόσο από το χημικό παράγοντα (φαινόμενα επιδιαλυτώσεως), όσο και από το φυσικό παράγοντα (διηλεκτρική σταθερά του μέσου). Οι δύο αυτοί παράγοντες στην περίπτωση των υδατομεθανολικών και υδατοακετονιτριλικών συστημάτων δρουν ανταγωνιστικά. Στις μικρές περιεκτικότητες σε οργανικό διαλύτη υπερισχύει η επίδραση του χημικού παράγοντα και έχουμε ελάττωση της σταθερότητας του συμπλόκου, ενώ στις μεγαλύτερες περιεκτικότητες παύει η επίδραση του χημικού παράγοντα και υφίσταται μόνο εκείνη του φυσικού παράγοντα και τότε έχουμε αύξηση της σταθερότητας του συμπλόκου με την αύξηση της % v/v περιεκτικότητας σε οργανικό διαλύτη. Στις περιεκτικότητες που παύει να δρα ο χημικός παράγοντας και υφίσταται μόνο ο φυσικός παράγοντας το pK του συμπλόκου είναι γραμμική συνάρτηση του αντίστροφου της διηλεκτρικής σταθεράς του διαλυτικού συστήματος.

Στην περίπτωση των υδατοδιοξανικών διαλυμάτων, λόγω μη αισθητής μεταβολής της εκτάσεως της επιδιαλυτώσεως με την προσθήκη του διοξάνιου, εκδηλώνεται από τις μικρές ακόμη περιεκτικότητες σε διοξάνιο η επίδραση μόνο του φυσικού παράγοντα.

References

1. Heyrovsky J. and Kuta J. : «*Principles of Polarography*» (Academic Press N.Y. and London 1966) p. 147.
2. Lingane J.J.: *J. Am. Chem. Soc.* **61**, 2099 (1939).
3. Lingane J.J. and Kolthoff I.M.: *J. Am. Chem. Soc.* **61** 825, 1045(1939).
4. Stackelberg M.: *Z. Elektrochem.* **45**, 466 (1939).
5. Tomes J.: *Coll. Czech. Chem. Commun.* **9**, 12, 81, 150 (1937).
6. Strehlow H., Mädrich O. and Stackelberg M.: *Z. Elektrochem.* **55**, 244 (1951).
7. Martens P.H. and Nangniot P., *Bull. inst. agron. et stas. recherches* **24**, 285 (1956).
8. Heyrovsky J. and Kuta J.: «*Grundlagen der Polarographie*» (Akademie Verlag, Berlin 1965) p. 187.
9. Lingane J.J.: *Chem. Rev.* **29**, 1 (1941).
10. Vlček A.A.: *Chem. listy* **48**, 1474 (1954). *Coll. Czech. Chem. Commun.* **20**, 400 (1955).
11. Jannakoudakis D. and Moutziz I.: *Chimika Chronika* **33A**, 7 (1968).
12. Jannakoudakis D. and Papanastassiou G.: *Chimika Chronika* **35**, 1 (1970).
13. Jannakoudakis D. and Papanastassiou G.: *Report of the fourth conference of the Greek Chemists*, Athens, May 1970.
14. Jannakoudakis D. and Papanastassiou G.: *Sci Annals Fac. Phys. & Mathem. Univ. Thessaloniki*, **11**, 497 (1971).
15. Jannakoudakis D. Theodoridou E. and Pelekourtsa A.: *Chimika Chronika New Series* **1**, 67 (1972).
16. Jannakoudakis D.: *Chimika Chronika* **30A**, 28 (1965).

CONCENTRATION AND STORAGE OF PEROXYACETYLNITRATE (PAN) FOR MOBILE FIELD MEASUREMENTS IN TROPOSPHERIC AIR

SOTIRIS GLAVAS AND ULRICH SCHURATH

Institut für Physikalische Chemie der Universität Bonn Wegelerstrasse 12, D-5300 Bonn. W. Germany

(Received October 25, 1982)

Summary

It is demonstrated that PAN in ambient air can be concentrated by cryotrapping, and stored at liquid nitrogen temperature. The analysis of PAN is performed after warming the evacuated sampler to room temperature by GC-ECD. In the warm sampler, which contains about 0.1 ml liquid water, PAN is lost at a rate of approximately $2.4 \times 10^{-4} \text{ s}^{-1}$, which is similar to the first order rate constant for homogeneous thermal decomposition of PAN in the gas phase. Therefore, hydrolysis of PAN in the wet sampler seems to be of minor importance. The concentration procedure is suitable for field measurements of very low PAN concentrations expected to be present in clean tropospheric air. Some preliminary results on PAN mixing ratios sampled in Bonn, Athens and Patras are reported.

Key words: Air cryosampling, Photochemical Air Pollution, Peroxyacetyl nitrate (PAN).

Introduction

Peroxyacetyl nitrate ($\text{CH}_3\text{COO}_2\text{NO}_2$, PAN) is a typical secondary air pollutant present in photochemical smog¹. Its phytotoxic effects on sensitive crops are well documented², but little is known about its long term effects on man and animals: PAN seems to be equally or less toxic than ozone³, but occurs in photochemical smog at mixing ratios 20 to 50 times less than ozone⁴. In spite of this unfavorable ratio, PAN is a less ambiguous indicator of photochemical air pollution than ozone, which is also a natural constituent of the atmospheric boundary layer, at mixing ratios between 20 and about 40 ppb in the clean troposphere⁵. This makes the distinction between "anthropogenic" and "natural" ozone rather ambiguous. However, because of analytical and calibration problems^{6,7,8} in the analysis of PAN in air by gas chromatography with electron capture detection (GC-ECD), ozone has become the preferred indicator of photochemical smog.

Recent one-dimensional model calculations^{9,10}, based on worldwide measurements of ethane, ethene, and NO_x , predict that PAN is also present as a trace constituent in clean tropospheric air. Due to the increased stability of PAN at low temperature^{11,12} its mixing ratio is expected to increase with altitude, and exceed that of all other NO_x compounds in the cold upper troposphere. So far, the predicted PAN concentrations (0.09 to 0.36 ppb in the upper troposphere) have not been verified by field measurements. The sensitivity of currently available ECD's would probably be adequate for its detection¹³, but the PAN measurements which have been reported in the literature were restricted to air samples collected in the immediate proximity of an immobile GC-ECD. Also, no suitable technique has been reported by which PAN can be sampled in the field, stored undecomposed, and transferred to a laboratory for analysis.

We have tested a simple but promising sampling technique meeting the requirements for remote field measurements, and present preliminary data on PAN concentrations in air samples collected at Bonn, Athens, and Patras.

Experimental

Air samples were injected into a dual column HP 5710A GC by means of gas tight glass syringes with teflon plungers (Precision Sampling Corporation, 2 to 5 ml volume). The GC was equipped with two identical glass columns of 60 cm length and 1.5 mm i.d., filled with 4.8 % QF-1 and 0.18 % diglycerol on chromosorb G-AW-DMCS (80-100 mesh). At a column temperature of 30.0 °C and a carrier gas flow rate of 30 ml min⁻¹, the PAN peak appeared 2.1 min after injection. One column was connected to a commercial ECD (HP, Nickel-63 constant current - variable pulse frequency mode). The detector temperature was 35 °C, and Argon containing 5 % CH_4 was used as carrier gas. The second column was followed by a catalytic NO_x converter, consisting of a heated quartz tube of 104 mm length and 3 mm i.d., filled with a mixture of molybdenum powder and coarsely ground spectrally pure graphitized carbon. The converter was conditioned with hydrogen at 335 °C for several hours, after which time nitrogen was used as carrier gas. At 335 °C, NO_2 , organic nitrites, PAN, and other organic nitrates were 100 % converted to NO with very little peak broadening. The NO peaks emanating from the converter column were measured with a dedicated chemiluminescence NO detector of special design. This GC- NO_x -detector¹⁴, which will be described in more detail in a future publication, is highly specific for convertible organic nitrogen compounds, NO, and NO_2 . Furthermore, it is strictly linear, and exhibits equal sensitivities for equal volume mixing ratios of all fully convertible nitrogen compounds. It could thus be calibrated conveniently with known concentrations of any of the above-listed compounds; usually a few 100 ppb NO or i-pentyl nitrite in nitrogen were used for calibration. The sensitivity of the ECD for PAN was then obtained by comparison, injecting identical air samples of roughly 20-100 ppb PAN into both columns, and measuring the exact PAN concentration with the GC- NO_x -detector.

A HP 3380A integrator/plotter was used for both detectors. Alternatively, concentrations were calculated from peak heights when the integrator failed because of detector noise, or gave unreliable results due to an ill-defined baseline. The sensitivity of the GC-NO_x-detector allowed 2 ppb PAN to be measured in 5 ml air, under the experimental conditions given. The signal-to-noise ratio of the ECD was more than 2 orders of magnitude higher, but background peaks of other electron capturing trace gases raised the practical detection limit in ambient air to about 0.1 ppb in 2 ml samples.

PAN in synthetic or ambient urban air was generated in cylindrical glass flasks of 4 liter volume, or in an evacuable all glass smog chamber of 425 liter volume, by irradiating air spiked with NO₂ and trans-2-butene with fluorescent UV lamps. The PAN concentrations obtained ranged from a few ppb up to several ppm, depending on the precursor concentrations.

The sampling procedure by which PAN in ambient air could be concentrated and stored for later analysis, which was tested in this work, is extremely simple: Cylindrical pyrex flasks of 100 ml volume, with a teflon stopcock and a vacuum tight silicone rubber septum, were immersed in liquid nitrogen. When the stopcock was opened, air started to condense in the pyrex flask. The procedure was terminated after 20 to 30 minutes by closing the stopcock. This time sufficed to collect 10 or more liters of air. The sample was transferred to the laboratory, where the liquefied air was gently pumped off, while keeping the flask fully immersed in the liquid nitrogen. It takes about 20-30 minutes to remove the volatile liquid. The amount of air collected is measured with a wet gas meter connected to the exhaust of the vacuum pump. The evacuated sample may be stored at liquid nitrogen temperature. For analysis, the pyrex flask is rapidly warmed to room temperature by flowing tap water, brought to atmospheric pressure with pure nitrogen, and analyzed directly by injecting a series of samples into the GC with gas tight syringes. Typical chromatograms of an ambient air sample which was concentrated 99 fold, are shown in figure 1. In the series of chromatograms obtained from one concentrated air sample, corrections were applied for sample dilution by repeated extractions of 2 to 5 ml air from the 100 ml flask. Typical concentration factors for ambient air samples ranged from 50 to 200.

Results and discussion

Linearity of the ECD

With the GC-NO_x-detector as reference standard it was possible, for the first time, to measure *directly* the sensitivity of the ECD down to 2 ppb PAN, which is the detection limit of the reference detector. This is in contrast to other calibration procedures reported in the literature, which have to rely on dilution of concentrated PAN samples^{5,6,7}. We found the sensitivity of our ECD to be constant ($\pm 5\%$) at 35° C between 1000 and 2 ppb PAN (1 ml samples). Increasing the ECD temperature to 100 °C reduced the sensitivity by a factor 4 at low PAN concentrations, presumably due to thermal decomposition. Above 100 ppb PAN the sensitivity of the hot ECD started to increase, reaching about half its low

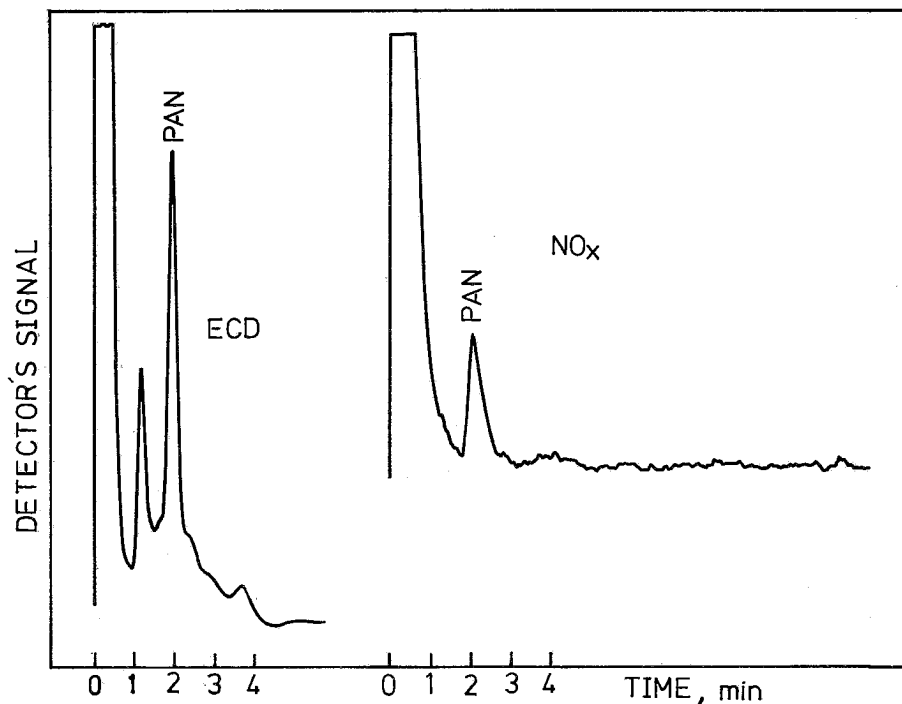
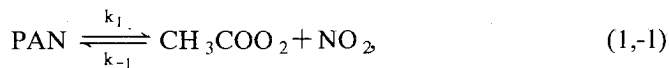


FIG. 1 : Gas chromatograms obtained with the ECD and the GC- NO_x -detector of an air sample containing 6 ppb in the concentrate. The corresponding mixing ratio of PAN in ambient air is 0.06 ppb.

temperature sensitivity at 1000 ppb. To eliminate these problems, all measurements reported below were done at a constant ECD temperature of 35 °C.

Evaluation of the sampling technique:

In field studies of stable trace gases like the halocarbons, grab sampling of air in stainless steel containers, for later analysis in the laboratory, has been quite successful. PAN, however, which exists in equilibrium with its radical fragments in the gas phase,



$$k_1 = 2.7 \times 10^{-4} \text{ s}^{-1} \text{ at } 298 \text{ K,}$$

cannot be stored in the gas phase at ambient temperature, because heterogeneous and homogeneous reactions of CH_3CO_3 , in competition with reaction (-1), result in irreversible decomposition. This can be avoided by cryosampling, provided that the frozen trace gas can be recovered quantitatively for GC analysis.

When ambient air is sampled by condensation at - 195 °C, as described in the

experimental part, approximately 0.1 ml ice is formed for every 10 liter of condensed air, yielding an equivalent amount of liquid water when warmed to room temperature for analysis. Expecting that the liquid water would cause PAN to hydrolyze in the sampling flask, several attempts were made to dry the air while it was being cryotrapped. It was found, however, that most if not all of the PAN was lost in the drying tube.

As it became clear that water could not be removed from the cryosamples, the disappearance rate of PAN was measured in wet pyrex flasks after warmup of cryotrapped air samples. It was found to be surprisingly slow, proceeding at a first order rate of typically $2.5 \times 10^{-4} \text{ s}^{-1}$. This is very close to the rate constant k_1 for the irreversible first order decay of PAN in the gas phase at room temperature (see above), which is observed in the presence of NO. Since NO is likely to be present in the wet pyrex sampler, it is quite possible that hydrolysis is in fact a negligible loss process for PAN in the sampler.

We then proceeded to show that our very simple cryotrapping method can be used for quantitative analysis. For the purpose, ambient air in the smog chamber was spiked with PAN in the concentration range 1-44 ppb, by injecting highly concentrated PAN samples which were prepared separately in a 4 liter pyrex flask

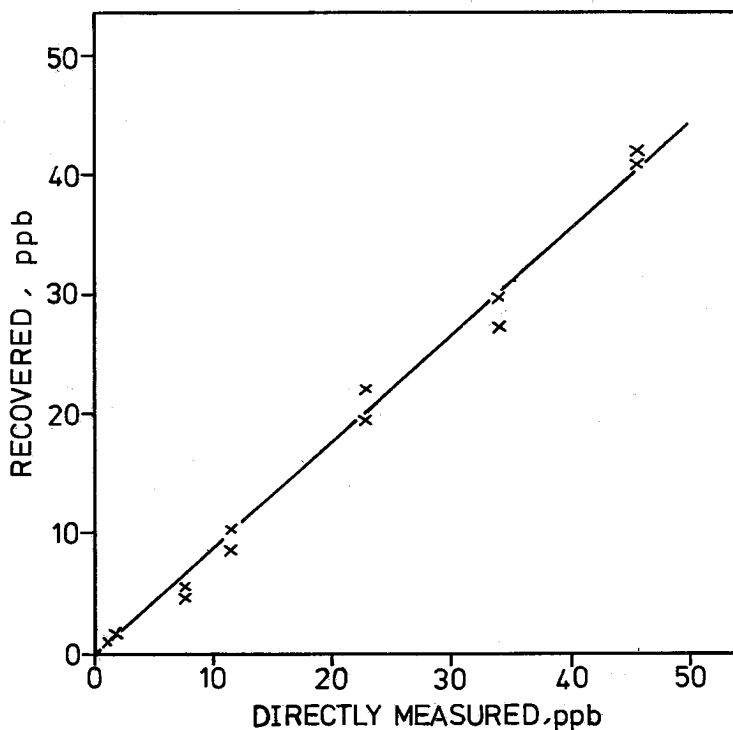


FIG. 2 : Plot of PAN recovered after the concentration procedure versus PAN measured directly.

by the photochemical method. After measuring the PAN concentration in the smog chamber, between 2 and 10 liters air were cryotrapped in a pyrex sampler. It was shown by further analyses that PAN was stable in the smog chamber during this procedure. The concentrates were treated as described in the experimental part, and analyzed by a series of injections into the GC. The results were evaluated by plotting the PAN recovered (= concentration in the pyrex sampler, divided by the concentration factor) versus PAN in the smog chamber, as shown in figure 2. The slope of the straight line, which fits the data within experimental scatter, is somewhat less than 45°, indicating that, on the average, 12 % PAN are lost in the whole procedure.

The reproducibility of the method was tested by collecting five ambient air samples in five pyrex samplers which were simultaneously exposed on a roof. The concentrates were analyzed using both the GC-NO_x-detector and the ECD. The results of the test are listed in Table I. The scatter of the data is considered to be

TABLE I: Reproducibility test. All five samples were collected simultaneously on 27 September, 1982.

Sample No.	Ambient mixing ratio of PAN (ppb); analysis by GC-NO _x -detector,	by ECD
1	0.025	0.042
2	0.038	0.051
3	0.059	0.038
4	0.048	0.051
5	0.044	0.043

mean values and deviations from the mean:

0.043 ± 0.016

0.045 ± 0.006

acceptable, in view of the low PAN concentrations present in the atmosphere, which was below our detection limit for direct analysis of air without preconcentration, but resulted in substantial peaks on both detectors after concentration (cf. figure 1). Since the evaluation of the PAN peak seen by the ECD is limited by background structure on the baseline, due to other trace gases with similar retention times (probably solvents used in neighbouring University Institutes), rather than by detector noise, considerably lower PAN concentrations can be measured in clean air by the concentration technique.

Although it can be assumed that samples stored at liquid nitrogen temperature are stable, the following rigorous test was made: A cryotrapped ambient air sample was warmed to room temperature for analysis, then rapidly immersed in liquid nitrogen again. This procedure was repeated on two consecutive days. The analyses yielded 0.060 ppb; 0.060 ppb; 0.062 ppb for the PAN concentration in the ambient air which had been trapped.

Field measurements

The first part of Table II lists a number of field measurements dating from 9 days in August and September 1982. The ozone concentrations, wind directions

TABLE II : Field measurements of PAN concentrations in Bonn, W. -Germany, and in Athens and Patras, Greece.

area	Date and time of sampling		Ozone (ppb)	PAN (ppb)	wind direction and speed (m/s)	
<i>Bonn</i>	18.08.82	16:00	43	0.10	SW	4.2
	18.08.82	18:20	35	0.09	SW	3.2
	19.08.82	15:30	48	0.17	WNW	4.0
	20.08.82	08:08	n.d.	0.05	SW	2.8
	21.08.82	15:00	n.d.	0.11	W	4.2
	23.08.82	11:00	n.d.	0.09	SSE	3.0
	24.08.82	13:45	30	0.12	W	2.3
	24.08.82	15:30	35	0.12	W	1.6
	26.08.82	08.20	0	0.04	S	2.1
	22.09.82	15:15	n.d.	0.11	NNW	2.5
	27.09.82	08:50	35 ⁺	0.03	SSE	3.4
	27.09.82	08:50	35 ⁺	0.04	SSE	3.4
	27.09.82	10:50	28	0.05	ESE	3.0
	27.09.82	10:50	28	0.03	ESE	3.0
	27.09.82	14:00	40	0.05 ⁺⁺	SE	3.3
<i>Athens</i>	14.09.82	17:00	n.d.	0.48	sunny, moderate to	
	15.09.82	16:00	n.d.	0.34	strong wind from	
	16.09.82	13:30	n.d.	0.78	N to NNW	
<i>Patras</i>	17.09.82	13:45	n.d.	0.07	moderate to strong wind from NNW, sunny	

⁺ozone measured at 10:15

⁺⁺average of five simultaneously taken samples.

Sampling sites : *Bonn*, Institut für Physikalische Chemie, University of Bonn.

Athens, Propylea, Acropolis.

Patras, Laboratory of Inorganic Chemistry, Downtown Patras.

and wind speeds are also given for the sampling time. The measuring period was sunny or slightly cloudy, with moderate to strong winds blowing predominantly from the W and SW. Air from these directions is advected over rural areas, and is usually very clean. Accordingly, the PAN and ozone concentrations were always very low, probably close to the rural background concentration in late summer.

The highest PAN and ozone values were measured on 19 August, probably due to advection of slightly more polluted air from the NW.

Table II also includes PAN mixing ratios in ambient air sampled in Athens and in Patras, Greece. The samples were permanently stored in liquid nitrogen in a dewar, and were transferred to Bonn by car for immediate analysis. The very low PAN mixing ratio in Patras, similar to the values in Bonn, is consistent with the low level of pollution in air advected from the NNW. The PAN mixing ratios found in Athens, though systematically higher than the other data, were sampled on clear windy days with efficient vertical mixing, and thus should be considerably lower than PAN mixing ratios during more typical photochemical smog episodes.

Summary and Conclusions

We have reported a simple concentration procedure for the measurement of PAN in ambient air. The method was evaluated with respect to reproducibility and PAN recovery, using a novel GC-NO_x-detector for calibrations of the ECD in the ppb range. The concentration procedure lowers the detection limit for PAN into the ppt range, and makes feasible the collection of samples in the field, far away from the laboratory where the analyses are carried out.

Περίληψη

Συμπύκνωση και διατήρηση δειγμάτων νιτρικού-υπεροξυακετυλίου (Peroxyacetylnitrate) PAN, για μετρήσεις του ατμοσφαιρικού αέρα μακριά από το εργαστήριο.

Παρουσιάζεται μέθοδος συμπύκνωσης δειγμάτων PAN στον ατμοσφαιρικό αέρα, του δεύτερου μετά το όζον πιο σημαντικού δευτερεύοντος φωτοχημικού οξειδωτικού, σε χαμηλή θερμοκρασία και διατήρηση αυτών των δειγμάτων σε υγρό άζωτο.

Η ανάλυση του PAN γίνεται μετά τη θέρμανση του δείγματος σε θερμοκρασία δωματίου και άντληση του δειγματολήπτη, με αέρια χρωματογραφία με ανιχνευτή συλλογής ηλεκτρονίων. Στο θερμό δειγματολήπτη που περιέχει περίπου 0,1 ml υγρό νερό, η απώλεια PAN γίνεται με ταχύτητα περίπου $2,4 \times 10^{-4} \text{ s}^{-1}$, που είναι παραπλήσια προς τη σταθερά ταχύτητας πρώτης τάξης της ομογενούς θερμικής διάσπασης του PAN στην αέρια φάση. Συνεπώς η υδρόλυση του PAN, στον δειγματολήπτη φαίνεται να είναι ασήμαντη.

Η μέθοδος συμπύκνωσης είναι κατάλληλη για μετρήσεις πεδίου πολύ χαμηλών τιμών PAN της τάξης μερικών ppt, σε καθαρό τροποσφαιρικό αέρα, αλλά και για δειγματοληψίες μακριά από το εργαστήριο όπου είναι εγκατεστημένος ο αέριος χρωματογράφος.

Οι δειγματοληψίες έγιναν βασικά στη Βόννη, Δυτ. Γερμανίας, στην Αθήνα και Πάτρα. Όλες οι μετρήσεις έγιναν κάτω από μετεωρολογικές συνθήκες που δεν ευνοούσαν τη δημιουργία φωτοχημικού νέφους. Οι μεγαλύτερες τιμές που μετρήθηκαν ήσαν στη Βόννη 0,16 ppb, στην Αθήνα 0,78 ppb και στην Πάτρα 0,07 ppb.

References

1. Stephens, E.R.: *Adv. Environ. Sci. Technol.* **1**, 119-147 (1969).
2. Taylor, O.C. : *J. Air Pollut. Control Assoc.* **19**, 347-352 (1969).
3. Krusse A., and Feron, V.J. : *VDI-Berichte* **270**, 101-109 (1977).
4. Nieboer, H. and van Ham, J. : *Atmos. Environ.* **10**, 115-120 (1976).
5. Singh, H.B., Ludwig, F.L. and Johnston, W.B. *Atmos. Environ.* **12**, 2185-2196 (1978).
6. Holdren, M.W. and Rasmussen, R.A. : *Environ. Sci. Technol.* **10**, 185-187 (1976).
7. Lonneman, W.A. : *Environ. Sci. Technol.* **11**, 194-196 (1977).
8. Watanabe, I. and Stephens, E.R. : *Environ. Sci. Technol.* **12**, 222-223 (1978).
9. Singh, H.B. and Hanst, P.L. : *Geophys. Res. Lett.* **8**, 941-944 (1981).
10. Aikin, A.C. Herman, J.R., Maier, E.J. and McQuillan, C.J. : *J. Geophys. Res.* **87**, 3105-3118 (1982).
11. Hendry, D.G. and Kenley, R.A. : *J. Am. Chem. Soc.* **99**, 3198-3199 (1977).
12. Cox, R.A. and Roffey, M.J. : *Environ. Sci. Technol.* **11**, 900-906 (1977).
13. Grennfelt, P., Samuelsson, U., Nielsen, T. and Thomsen, E.L. Proceedings of the second European Symposium *Physico-Chemical Behaviour of Atmospheric Pollutants*, D. Reidel 1982, p. 619-624.
14. Richthofen, A. von, Diplomarbeit, Bonn 1982.

Acknowledgements

This work was supported in part by the Minister für Wissenschaft und Forschung des Landes Nordrhein-Westfalen. One of us (S.G.) wishes to thank the International Bureau of the Kernforschungsanlage in Jülich, W. Germany, for a grant.

SYNTHESE SOUS PRESSION D'UNE SERIE NOUVELLE DE PEROVSKITES DE TERRE RARE DE FORMULE $TCu_{3-x}Mn_{4+x}O_{12}$

D. SAMARAS

Laboratoire de Science des Métaux Faculté Polytechnique Université "Aristote" Thessaloniki Grèce

(Received February 7, 1983)

Résumé

Une série nouvelle d'oxydes mixtes de cuivre, manganèse et terre rare de formule générale $TCu_{3-x}Mn_{4+x}O_{12}$ (T = terre rare ou yttrium), à structure dérivant de celle de la perovskite ($a \approx 7,30$ Å, groupe d'espace $Im3$, $Z = 2$), a été synthétisée sous pression. La composition est fortement influencée par la température et la pression utilisées pour la synthèse. Le paramètre de substitution d'ions Cu^{2+} par des ions Mn^{3+} en synthèse hydrothermale varie entre $x = 0$ pour 500 °C/3kbar et $x = 0,75$ pour 750 °C/1kbar. Le résultat est attribué à l'action cristalochimique de la pression.

Key words: High pressure synthesis, Hydrothermal synthesis, Rare-earth perovskites, Magnetic oxides.

Introduction

Les composés de formule générale $[AC_3]B_4O_{12}$ possèdent une structure qui constitue une déformation cubique de la structure du type pérovskite avec un paramètre de maille double de celui de la perovskite ($a \approx 7,30$ Å, groupe d'espace $Im3$, $Z = 2$). Le doublement du paramètre de maille est dû à l'ordre entre les cations A et C, lui même provenant de l'enchaînement particulier des octaèdres (BO_6); en effet les chaînes d'octaèdres se propagent en zig-zag, l'angle d'inclinaison par rapport à la droite étant voisin de 20° . Cette disposition des octaèdres entraîne une distorsion importante de $3/4$ des sites à coordination XII de la structure perovskite idéale: les cations C dans les composés $[AC_3]B_4O_{12}$ occupent des sites à coordination de quatre voisins formant un carré.

Ce type de coordination convient parfaitement à des cations tels que Cu^{2+} ou Mn^{2+} (spin haut), bien connus pour leur tendance à donner naissance à un effet Jahn-Teller coopératif important. C'est ainsi que deux sous-séries ($C = Cu^{2+}$ ou Mn^{3+}) ont été préparées jusqu' à présent¹⁻¹⁰. Les sites A, à coordination XII sous forme d'icosaèdre, peuvent être occupés par tout cation ionique important, ou

même des lacunes¹¹, indépendamment de sa charge, l'équilibre électrostatique pouvant être assuré par la valence du cation B.

Dans le présent travail est exposée la synthèse des composés de la série $[\text{TCu}_3]\text{Mn}_4\text{O}_{12}$ (T = terre rare ou Y). L'existence de solutions solides entre les deux sous-séries (C = Cu^{2+} ou Mn^{3+}) étant déjà signalée¹²⁻¹⁴, une étude systématique a été menée sur la possibilité de synthèse de composés de formule $\text{T}(\text{Cu}_{3-x}^{2+}\text{Mn}_x^{3+})(\text{Mn}_{3-x}^{4+}\text{Mn}_{1+x}^{3+})\text{O}_{12}$ par ajustage adéquat des conditions de température et de pression utilisées lors de la synthèse. Les perovskites $[\text{AC}_3]\text{B}_4\text{O}_{12}$ présentant des propriétés magnétiques d'un intérêt technologique certain^{4,5,7-9,12-14} la recherche de composés non stoechiométriques a été entreprise en vue de l'étude de l'influence de la terre rare et de la concentration en cuivre et manganèse sur les propriétés magnétiques de la série.

Synthèses sous haute pression et caractérisation aux rayons X

Dans le cas où une réduction du cation destiné à occuper le site B de la formule $[\text{AC}_3]\text{B}_4\text{O}_{12}$ n'est pas à craindre, on peut procéder à la synthèse des composés correspondants par frittage du mélange des constituants dans des proportions stoechiométriques à des températures voisines de 1000 °C. C'est le cas en particulier de la série des titanates¹¹ et rhuthéniates^{14,15} cuivriques. Par contre, une réduction de Mn^{4+} étant attendue aux températures nécessaires à la synthèse, nous avons été conduits à appliquer une pression pour élargir en température le domaine de stabilité de ce cation.

Toute la série des manganites cuivriques de terres rares a été obtenue par calcination du mélange de l'oxyde de terre rare avec CuO et MnO_2 dans des proportions stoechiométriques à des températures entre 1000° et 1200 °C sous 50 Kbar dans un appareil de type Belt X. Le milieu oxydant provient de la réduction de 1/3 des ions Mn^{4+} en Mn^{3+} pour satisfaire l'équilibre de la formule.

Tous les composés ont été examinés aux rayons X à l'aide d'une chambre à focalisation de Guinier utilisant la radiation K_α du fer. Un étalon de Si a été incorporé afin d'éliminer les erreurs dues à une imprécision dans la détermination de l'origine. Tous les clichés ont été indexés dans une maille cubique centrée. Les paramètres de maille affinés sont consignés au tableau I. Sur le même tableau sont fournis les paramètres de maille de la série de composés préparés par synthèse hydrothermale à 600 °C/1,5 kbar. Sur le tableau II est présenté un diagramme de rayons X d'une préparation typique de $\text{YCu}_3\text{Mn}_4\text{O}_{12}$ à ces conditions de synthèse.

Préparation en synthèse hydrothermale

La recherche des conditions optimales de synthèse hydrothermale a été entreprise sur les composés contenant le néodyme et l'yttrium. En utilisant comme produits de départ les oxydes correspondants dans des proportions stoechiométriques, différents solvants, tels que H_2O , HCl , HNO_3 et HClO_3 ont été essayés. La synthèse, effectuée à 600 °C et des pressions comprises entre 1 et 2 kbar dans des tubes scellés d'or, fournit le composé recherché avec un rendement médiocre. Les meilleurs rendements (15 - 20%) ont toutefois été obtenus avec comme solvant l'eau distillée additionnée d'acide nitrique, quand le pH de la solution était inférieur

TABLEAU I : Paramètres de maille des composés de la série $[\text{TCu}_3]\text{Mn}_4\text{O}_{12}$

Oxyde de T.R.	Paramètre de maille en Å ($\pm 0,001$)	
	HP ¹	SH ²
La ₂ O ₃	7,355	7,322
CeO ₂	7,319	7,299
Pr ₆ O ₁₁	7,320	7,293
Nd ₂ O ₃	7,340	7,305
Sm ₂ O ₃	7,298	7,295
Eu ₂ O ₃	7,292	7,284
Gd ₂ O ₃	7,278	7,282
Tb ₄ O ₇	7,255	7,253
Dy ₂ O ₃	7,256	7,266
Ho ₂ O ₃	7,250	7,262
Er ₂ O ₃	7,249	7,262
Tm ₂ O ₃	7,246	
Yb ₂ O ₃	7,237	7,253
Lu ₂ O ₃	7,237	7,248
Y ₂ O ₃	7,252	7,263

(1) HP : 1000°- 1200°C/50 Kbar, frittage

(2) SH : 600°C/1,5 Kbar, synthèse hydrothermale.

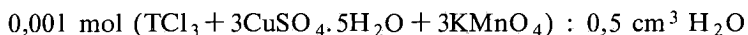
TABLEAU II : Diagramme de rayons X (chambre de focalisation 360 mm, λFeK_α) d'une préparation de $\text{YCu}_3\text{Mn}_4\text{O}_{12}$ à 600°C/1,5 Kbar.

hkl	I _{ob}	d _{ob}	d _{calc}
110	w	5,138	5,136
200	vw	3,631	3,632
211	m	2,965	2,965
220	vs	2,568	2,568
310	m	2,298	2,297
222	m	2,097	2,097
321	m	1,9611	1,9414
400	s	1,8153	1,8160
411 } 330 }	vw	1,7128	1,7121
332	vw	1,5483	1,5487
422	vs	1,4831	1,4827

à 4, et avec HClO_3 . Les phases parasites les plus importantes étaient le spinelle CuMn_2O_4 et les oxydes de départ CuO et MnO_2 .

L'ensemble de ces observations indiquant (a) une protection insuffisante des ions Mn^{4+} contre la réduction, (b) la mauvaise solubilité des oxydes et (c) l'importance du pH acide, une deuxième série de synthèses a été effectuée en utilisant comme produits de départ des sels censés plus solubles, tels que TCl_3 , $\text{CuSO}_4 \cdot 5\text{H}_2\text{O}$ ou CuCl_2 et KMnO_4 . Dans ce milieu, très oxydant en raison de la réduction des ions Mn^{7+} en Mn^{4+} et Mn^{3+} , des rendements de l'ordre de 70% ont été obtenus avec comme solvant l'eau distillée. Il n'a pas été nécessaire d'ajouter du HNO_3 , l'acidité du milieu étant assurée par les sels cuivriques en solution. Il a été trouvé que la composition du mélange de départ pouvait varier dans des limites assez larges, sans influence sur le rendement, à condition que le $\text{CuSO}_4 \cdot 5\text{H}_2\text{O}$ s'y trouve en excès.

L'influence sur le rendement de la température et de la pression utilisées n'est pas négligeable quoique son importance se manifeste surtout sur l'état de cristallisation. Les meilleurs résultats ont été obtenus pour des températures de synthèse entre 600° et 750°C , cette dernière température conduisant à un produit formé de cristaux cubiques de plusieurs dixièmes de mm pour Y, quelques centièmes de mm pour Nd. La pression, liée à la température, ne peut pas être inférieure à 1 kbar pour les températures du haut de gamme (700° - 750°C) alors qu'à 500°C la synthèse peut être réalisée à 800 bar. Enfin, le rapport solvant/soluté s'avère très décisif sur l'état de cristallisation. Les meilleurs résultats ont été obtenus pour une composition typique.



Dans toutes les expériences de synthèse hydrothermale avec l'yttrium la pression a été appliquée dès la température ambiante et maintenue à sa valeur lors de la montée en température. Les produits de synthèse ont été isolés par tri magnétique et purifiés par lavages successifs dans l'acide oxalique et le chlorure d'ammonium.

Composition des produits

Le paramètre de maille, déterminé à l'aide de clichés de rayons X sur chambre à focalisation, varie dans des limites assez importantes selon les conditions de température et de pression, aussi bien pour les échantillons fabriqués en synthèse hydrothermale que pour ceux obtenus par frittage sous haute pression (fig. 1,2). Ce résultat semble indiquer que la composition du produit varie en fonction de la température et de la pression de préparation. En effet, l'ion Mn^{3+} , de rayon ionique¹⁶ comparable à celui de Cu^{2+} et susceptible de donner naissance à des polyèdres de coordination déformés par effet Jahn-Teller, pourrait remplacer partiellement l'ion Cu^{2+} dans les sites C de la formule $[\text{AC}_3]\text{B}_4\text{O}_{12}$. La formule du produit doit, dans ce cas, s'écrire $\text{T}(\text{Cu}_{3-x}^{2+}\text{Mn}_x^{3+})(\text{Mn}_{3-x}^{4+}\text{Mn}_{1+x}^{3+})\text{O}_{12}$. Le paramètre de sa maille est très sensible au paramètre de substitution x en raison de la taille très différente des ions Mn^{3+} et Mn^{4+} occupant les sites octaédriques de la structure (Mn^{3+} : $r=0,64 \text{ \AA}$; Mn^{4+} : $r=0,54 \text{ \AA}$). Une augmentation de la température de

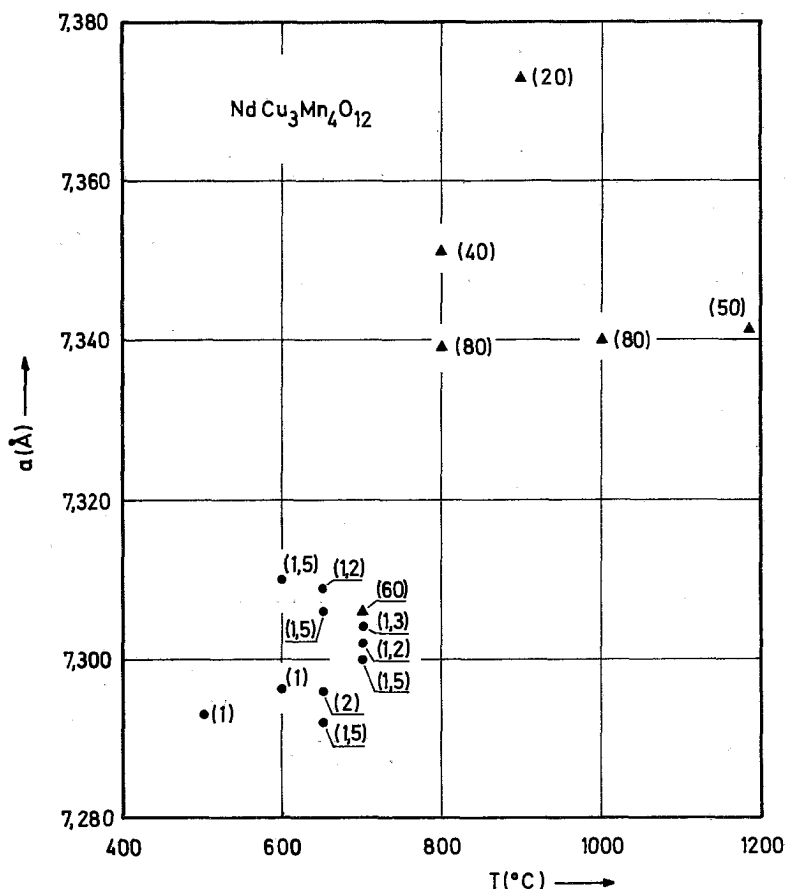


FIG. 1 : Paramètres de maille des échantillons de $\text{NdCu}_3\text{Mn}_4\text{O}_{12}$ préparés en synthèse hydrothermale (●) et sous haute pression (▲) en fonction de la température de préparation (entre parenthèses la pression en Kbar).

synthèse, favorisant la réduction de Mn^{4+} , conduit à un produit riche en Mn^{3+} ayant une maille plus volumineuse. C'est précisément ce que l'on observe aussi bien pour le composé du néodyme que pour celui de l'yttrium. Quant à l'influence de la pression appliquée, incertaine pour le composé du néodyme, elle est très nettement marquée pour le composé de l'yttrium: par son effet protecteur sur le degré d'oxydation de Mn^{4+} elle conduit à des mailles plus petites.

Les expériences complémentaires de synthèse hydrothermale du composé de Y sous une pression de 80 Kbar ont toutes abouti à un produit ayant un paramètre de maille identique, aux erreurs expérimentales près, à celle du produit fabriqué à $500\text{ °C}/3\text{ Kbar}$ ($a = 7,252(1)\text{ Å}$, fig. 2). Le même paramètre de maille a été obtenu pour les produits fabriqués par frittage des oxydes sous très haute pression (50-80 Kbar). La possibilité d'obtention de la composition nominale $\text{YCu}_3\text{Mn}_4\text{O}_{12}$

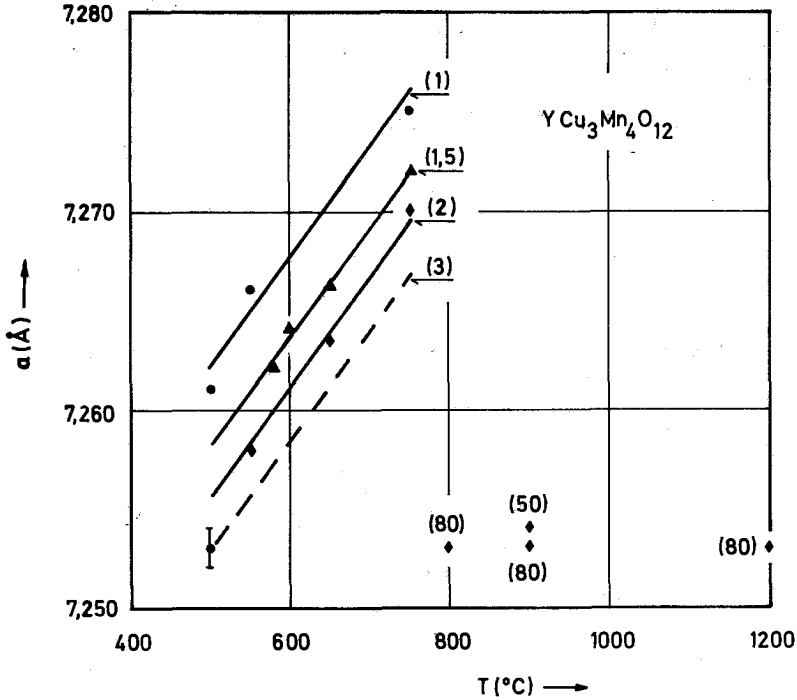


FIG. 2 : Paramètres de maille des échantillons de $YCu_3Mn_4O_{12}$ préparés en synthèse hydrothermale et sous haute pression en fonction de la température de synthèse (en paramètre la pression en Kbar):

($x = 0$) dans les autoclaves courants de synthèse hydrothermale ($P < 4$ Kbar) a ainsi été établie.

Ces résultats ont été complétés par analyse chimique à l' aide de la microsonde de Castaing effectuée sur des monocristaux cubiques de $YCu_3Mn_4O_{12}$ de 0,1 mm

TABLEAU III : Composition des composés $Y(Cu_{3-x}Mn_x)Mn_4O_{12}$ en fonction des conditions de préparation

Exp	T °C	Conditions P Kbar	a		Composition at %		
			Å ($\pm 0,001$)	Y	Cu	Mn	x
IX	500	3	7,253	4,8	14,8	20,4	0,06
VII	500	3	7,252	4,9	15,0	20,1	0,01
HPD	900	50	7,254	5,1	14,6	20,4	0,08
II	600	1,5	7,264	4,7	13,1	22,2	0,41
IV	750	2	7,270	5,4	11,7	22,9	0,51
VI	750	1	7,275	5,3	11,1	23,5	0,75

de côté (tableau III). Il en ressort que: (a) les produits possédant le paramètre de maille minimum correspondent à la composition nominale; (b) le paramètre de substitution peut atteindre un maximum $x = 0,75$ pour la préparation à $750^\circ\text{C}/1$ Kbar; (c) les produits ayant le même paramètre de maille correspondent à la même composition. Cette dernière constatation permet de tracer la courbe de la figure 3, reliant la composition au paramètre de maille.

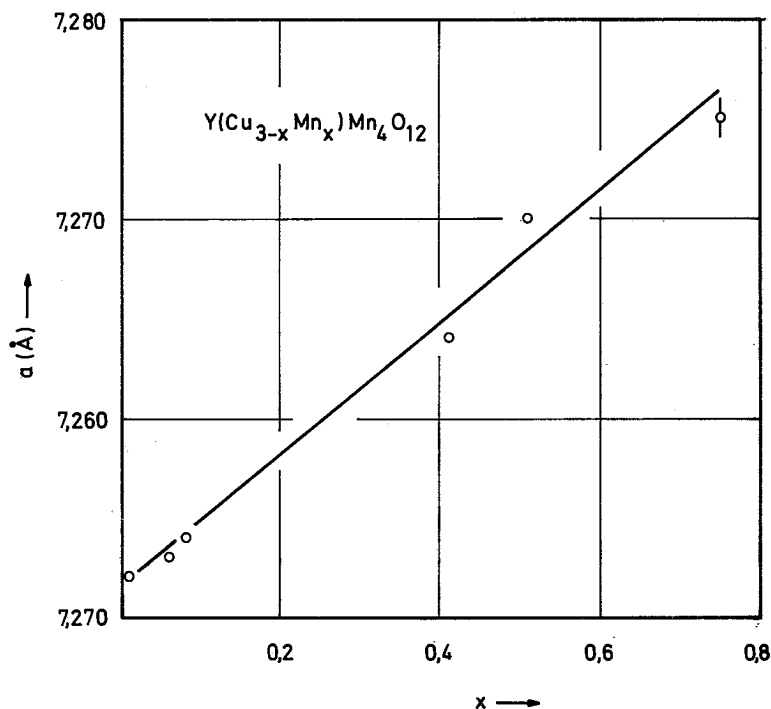


FIG. 3 : Variation du paramètre de maille des solutions solides $\text{Y}(\text{Cu}_{3-x}\text{Mn}_x)\text{Mn}_4\text{O}_{12}$ en fonction du paramètre de substitution x .

Discussion

La variation du paramètre de maille en fonction du numéro atomique de la terre rare (fig. 4) présente une allure régulière, aussi bien pour les produits fabriqués par frittage à haute pression que pour ceux fabriqués par synthèse hydrothermale. Cependant, des anomalies importantes apparaissent pour les composés de Ce, Pr et Tb dont les paramètres de maille sont sensiblement inférieurs à ceux que l'on serait en droit d'attendre. Une explication à cela peut être fournie par la variation du paramètre de maille avec la composition chimique: le potentiel d'oxydoréduction plus important pour ces terres rares conduit, pour

les mêmes conditions de préparation, à une formule moins riche en Mn^{3+} et un paramètre de maille inférieur.

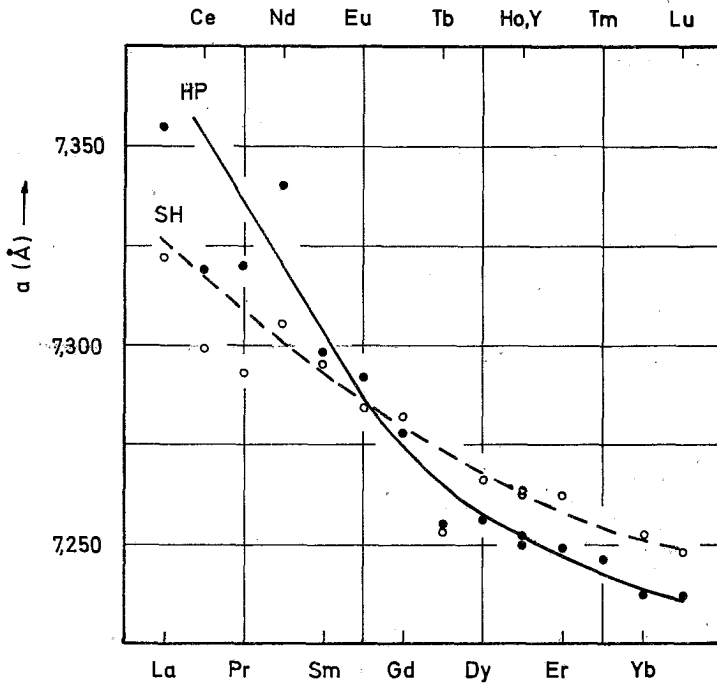


FIG. 4 : Variation de la maille des composés $\text{TCu}_3\text{Mn}_4\text{O}_{12}$ préparés en synthèse hydrothermale (SH : - - o -) et sous haute pression (HP : -●-) en fonction du numéro atomique de la terre rare.

L'obtention de la composition nominale $\text{YCu}_3\text{Mn}_4\text{O}_{12}$ nécessite l'application d'une pression de 3 Kbar à la température de 500 °C. Un défaut de pression et/ou une augmentation de la température de synthèse conduit à une réduction importante de l'ion manganèse sur les sites octaédriques B de la structure. Par contre, le composé $\text{ThCu}_3\text{Mn}_4\text{O}_{12}$ préparé à 600 °C/1,5 Kbar, possède la composition nominale⁶. Très vraisemblablement, l'apparition d'ions Mn^{3+} en excès dans $\text{YCu}_3\text{Mn}_4\text{O}_{12}$ préparé sous les mêmes conditions est liée au rayon moyen du cation destiné à occuper le site B. Dans $\text{ThCu}_3\text{Mn}_4\text{O}_{12}$ le site B contient des ions Mn^{3+} et Mn^{4+} en proportions égales et le rayon de l'ion moyen de ce site est de 0,59 Å. Or, pour le composé " $\text{YCu}_3\text{Mn}_4\text{O}_{12}$ " préparé à 600 °C/1,5 Kbar le paramètre de substitution $x = 0,41$ et le rayon de l'ion moyen du site B est $r = 0,57$ Å. Pour $\text{CaCu}_3\text{Mn}_4\text{O}_{12}$ préparé dans les mêmes conditions le rayon de l'ion moyen sur le site B est $r = 0,56$ Å. Ce résultat est en très bon accord avec ce que nous déterminons, compte tenu de la légère mais non négligeable influence du rayon du cation en site A sur les dimensions de la maille. Nous estimons que la pression nécessaire

pour obtenir la composition nominale $YCu_3Mn_4O_{12}$ à $600^\circ C$ doit être de l'ordre de 10 Kbar.

Si la pression appliquée, à une certaine température, est inférieure à celle nécessaire pour l'obtention d'une composition déterminée, la taille du cation en site B s'adapte par réduction partielle de Mn^{4+} en Mn^{3+} . La compensation des charges impose alors la présence d'ions Mn^{3+} sur le site C. Cette adaptation par réduction a manifestement lieu dans toute la série de composés $TCu_3Mn_4O_{12}$. Elle est impossible dans $CaCu_3Ge_4O_{12}$; c'est pourquoi la préparation de ce composé ne peut se faire que sous très haute pression (50 Kbar). C'est également le cas de $CaCu_3Cr_4O_{12}$ où la réduction de Cr^{4+} en Cr^{3+} est possible mais l'introduction de Cr^{3+} sur le site C est malaisée car cet ion n'est pas connu pour donner naissance à un effet Jahn-Teller coopératif.

Alors qu'une pression de 50 Kbar est suffisante pour la fabrication du composé de Y stoechiométrique, cette même pression s'avère nettement insuffisante pour le composé correspondant de Nd. En effet, ce dernier fabriqué à $1200^\circ C/50$ Kbar possède une maille supérieure à celui fabriqué à $600^\circ C/1,5$ Kbar (fig. 2) et son écart de la composition stoechiométrique doit être important. Ce phénomène est très vraisemblablement lié à la taille du cation occupant le site A. L'ion Nd^{3+} ayant un rayon ionique plus important que Y^{3+} doit provoquer une légère dilatation des octaèdres BO_6 . Dès lors l'introduction du même cation sur le site B nécessitera une pression plus importante pour le composé de Nd. A température égale, la pression nécessaire pour fabriquer un composé avec un paramètre de substitution x donné sera d'autant plus grande que le rayon de l'ion T^{3+} est grand. Le composé de Nd fabriqué dans les conditions extrêmes de synthèse hydrothermale en autoclave ($500^\circ C/3$ Kbar) ne doit pas être stoechiométrique.

Summary

Synthesis under pressure of a new series of rare earth perovskites with formula $TCu_{3-x}Mn_{4+x}O_{12}$.

A new series of mixed oxides of copper, manganese and rare earth, formula $TCu_{3-x}Mn_{4+x}O_{12}$ (T = rare earth or yttrium) with a perovskite-like structure ($a=7,30 \text{ \AA}$, space group $Im3$, $Z=2$) has been synthesised under pressure. The composition is strongly influenced by the synthesis's pressure and temperature. The substitution parameter of Cu^{2+} ions by Mn^{3+} , for samples prepared by hydrothermal synthesis, varies between $x=0$ for $500^\circ C/3$ Kbar and $x=0,75$ for $750^\circ C/1$ kbar. The result is attributed to the crystal-chemical action of the pressure.

Περίληψη

Σύνθεση υπό πίεση μιας νέας σειράς περοβσκιτών σπανίων γαιών με χημικό τύπο $TCu_{3-x}Mn_{4+x}O_{12}$

Η κρυσταλλική δομή των ενώσεων γενικού χημικού τύπου $|AC_3|B_4O_{12}$

αποτελεί μία παραμόρφωση της δομής τύπου περοβσκίτη με σταθερή κυψελίδα ($a \approx 7,30 \text{ \AA}$) διπλάσια από αυτήν του περοβσκίτη. Ο διπλασιασμός οφείλεται στην τάξη ανάμεσα στα κατιόντα A και C: τα ιόντα C βρίσκονται σε θέσεις με αριθμό σύνταξης IV σε μορφή τετραγώνου, σύνταξη που προσφέρεται για κατάληψη από κατιόντα που προκαλούν παραμόρφωση του τύπου Jahn-Teller (Cu^{2+} , Mn^{3+})¹⁻¹⁰.

Μια νέα σειρά μικτών οξειδίων χαλκού, μαγγανίου και λανθανιδών με χημικό τύπο $\text{TCu}_3\text{Mn}_4\text{O}_{12}$ (T = σπάνια γαία ή ύτριο) παρασκευάστηκε σε συνθήκες υψηλής πίεσης ($800^\circ - 1200^\circ\text{C}/20 - 80 \text{ kbar}$) και με υδροθερμική σύνθεση ($500^\circ - 750^\circ\text{C}/1-3 \text{ kbar}$). Η συμμετρία τους είναι κυβική και η σταθερή της κυψελίδα τους κυμαίνεται από $a = 7,237 \text{ \AA}$ (T = Lu) μέχρι $a = 7,355 \text{ \AA}$ (T = La) (πιν. I). Η σταθερή της κυψελίδα εξαρτάται, για την ίδια σπάνια γαία, από τις συνθήκες πίεσης - θερμοκρασίας που χρησιμοποιήθηκαν (πιν. III), γεγονός ενδεικτικό του σχηματισμού στερεών διαλυμάτων του τύπου $\text{T}(\text{Cu}_{3-x}^{2+}\text{Mn}_x^{3+})(\text{Mn}_{1+x}^{3+}\text{Mn}_{4-x}^{4+})\text{O}_{12}$. Η χημική ανάλυση έδειξε ότι: (α) δείγματα που παρασκευάζονται σε $500^\circ\text{C}/3 \text{ kbar}$ έχουν τη μικρότερη κυψελίδα και αντιστοιχούν σε $x = 0$, (β) το ποσοστό Mn στο δείγμα αυξάνει με τη θερμοκρασία σύνθεσης και ελαττώνεται με την πίεση, (γ) η μέγιστη υποκατάσταση Cu από Mn συμβαίνει για $750^\circ\text{C}/1 \text{ kbar}$, σε ποσοστό 25%, (δ) δείγματα με την ίδια κυψελίδα έχουν την ίδια σύσταση, γεγονός που επιτρέπει την παρασκευή δειγμάτων ελεγχόμενης σύστασης με κατάλληλη επιλογή των συνθηκών πίεσης-θερμοκρασίας.

Σύγκριση με άλλα μέλη της οικογένειας μικτών οξειδίων του τύπου $\text{AC}_3\text{B}_4\text{O}_{12}$ ^{5,6,12,17} επιτρέπει την ερμηνεία του αποτελέσματος με τη χημική δράση της πίεσης, η οποία, εξασφαλίζοντας την εισαγωγή κατιόντος μικρότερης ακτίνας στη θέση B επιτρέπει τη διατήρηση υψηλότερου μέσου βαθμού οξειδωσης για το μαγγάνιο.

References

1. M. Marezio, P.D. Dernier, J. Chenavas, J.C. Joubert : *J. Solid State Chem.*, **6**, 16 (1973).
2. B. Bochu, J. Chenavas, J. C. Joubert, M. Marezio : *J. Solid State Chem.* **11**, 88 (1974).
3. J. Chenavas, J.C. Joubert, M. Marezio, B. Bochu : *J. Solid State Chem.* **14**, 25 (1975).
4. J. Chenavas, J.J. Capponi, J.C. Joubert, M. Marezio : *Proceedings of the 4th International Conference on High Pressure*, Kyoto 1974; p 176.
5. A. Collomb, J. Chenavas, J.C. Joubert, M.N. Deschizeaux, B. Bochu, M. Marezio : *Proceedings of the 20th Annual Conference on Magnetism and Magnetic Materials*, San Francisco 1974, p. 368.
6. M.N. Deschizeaux, J.C. Joubert, A. Vegas, A. Collomb, J. Chenavas, M. Marezio *J. Solid State Chem.* **19**, 45 (1976).
7. A. Collomb, D. Samaras, G. Fillion, M.N. Deschizeaux, J.C. Joubert : *J. Mag. Mag. Mater.* **8**, 77 (1978).
8. A. Collomb, D. Samaras, B. Bochu, J. Chenavas, M.N. Deschizeaux, J.C. Joubert : *Physica*, **86-88B**, 927 (1977).

9. M.N. Deschizeaux, B. Bochu, J.C. Joubert, G. Fillion, J. Chenavas, A. Collomb, D. Samaras, M. Marezio : *J. Physique* **38** C1-103 (1977).
10. B. Bochu, M.N. Deschizeaux, J.C. Joubert, J. Chenavas, A. Collomb, J.P. Levy, M. Marezio, D. Samaras, G. Fillion : *J. Physique* **38** C1-95 (1977).
11. B. Bochu, M.N. Deschizeaux, J.C. Joubert, A. Collomb, J. Chenavas, M. Marezio : *J. Solid State Chem.*, **29**, 291 (1979).
12. A. Collomb, D. Samaras, J. Chenavas, M. Marezio, J.C. Joubert, B. Bochu, M.N. Deschizeaux : *J. Mag. Mag. Mater.* **7**, 1 (1978).
13. B. Bochu, J.C. Joubert, A. Collomb, B. Ferrand, D. Samaras : *J. Mag. Mag. Mater.* **15-18**, 1319 (1980).
14. J.C. Joubert, B. Bochu, M.N. Deschizeaux, A. Collomb, M. Marezio, J. Chenavas : *Proceedings of the International Conference on Ferrites*, Kyoto 1980.
15. M. Labeau, B. Bochu, J.C. Joubert, J. Chenavas : *J. Solid State Chem.* **33**, 257 (1980).
16. R.D. Shanon : *Acta Cryst. A* **32**, 751 (1976).
17. Y. Ozaki, M. Ghedira, J. Chenavas, J.C. Joubert, M. Marezio : *Acta Cryst. B* **33**, 3615 (1977).

SHORT PAPER

Chimika Chronika, New Series, 12, 111-116 (1983)

A SIMPLE METHOD FOR THE DETERMINATION OF GAS PERMEABILITY VALUES OF VARIOUS FILMS USED IN FOOD AND DRUG PACKAGING APPLICATIONS

M.G. KONTOMINAS, E. HATZIDIMITRIOU and E.K. VOUDOURIS
Dept. of Food Chemistry Univ. of Ioannina, Ioannina, Greece.

(Received June 14, 1982)

Key Words : Plastic films, permeability, CO₂ determination.

Introduction

The use of gas storage to increase the storage life of fruits, mainly apples and pears, packaged in plastic films is a common practice today^{1,2}. Furthermore gas storage has been employed recently to accelerate the ripening process of products such as bananas^{3,4,5}.

On the other hand, attention has been focused on the possibility of increasing the storage life of several oxygen-sensitive drugs, packaged in blister plastics. In all the above cases the permeability characteristics of the plastic films used, have been determined using various methods^{6,7,8,9,10}. The common feature of these methods is the use of the «permeability cell»⁶ an apparatus enabling the determination of gas permeability values of no more than two plastic films simultaneously.

The proposed modified method in this paper employs a series of glass mason jars instead of the permeability cell, which enable the determination of gas permeability values of 10-15 samples simultaneously.

Experimental

Principle of method

Pouches, formed from the plastic films are placed in an appropriately closed

system. The respective gas (CO_2 , O_2) is then passed through the system and the amount permeated into the pouch is quantified using Gas Chromatography.

Description of Method

Rectangular pieces of films (16×12)cm were cut from the respective rolls supplied by Enviro Systems Inc. N.J. U.S.A. and pouches having a surface area of (7×10)cm were constructed by heat sealing all four ends of film pieces. An inert plastic spacer made of styrene foam was introduced into the pouch before sealing, to aid sampling with a syringe. A silicon septum was then formed on one side of the pouch in order to monitor gas composition changes inside the pouch.

A Varian 3700 gas chromatograph equipped with a thermal conductivity detector was used for the quantification of CO_2 concentration within the pouch.

Initial CO_2 concentrations (W/V) inside the pouches were established by flushing 100% N_2 gas through the pouches. Following flushing and initial reading, the pouches were placed into a series of glass Mason jars (Figure 1) of 1 lt capacity, 1 pouch per jar, the jars were sealed and 100% CO_2 gas flushed continuously through the system to maintain the CO_2 level outside the pouches at 100%. Samples were taken at predetermined intervals by disconnecting one jar from the system, opening it, removing the pouch, and withdrawing 0.5 ml samples through the septum using a 0.5 ml gas tight syringe, equipped with a one way luer lock valve. The sample was introduced into the gas Chromatograph and the response was recorded.

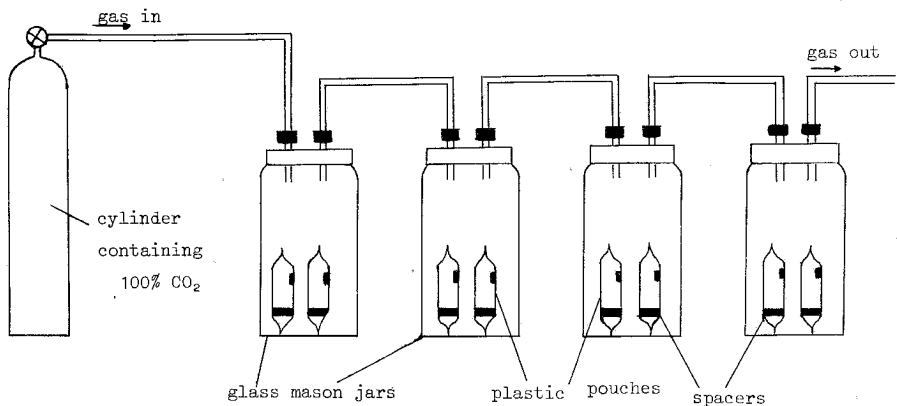


FIG. 1 : Scheme showing the assembly of Mason jars, containing the plastic pouches, for the measurement of CO_2 permeation rates of plastic pouches.

Quantification of CO_2 was accomplished using a standard curve, constructed daily by injecting known aliquots of various concentrations of 100% CO_2 .

Gas chromatographic conditions were as follows :

Column : Silica gel $2\text{m} \times 0.6$ cm st. steel, 60-80 Mesh

Column Temperature : 125°C
 Inj. port » : 130°C
 Detector » : 225°C
 Carrier gas : Helium 30 ml/min.

Procedure to determine the volume of the pouch

After measuring the % CO₂ concentration inside the pouch at time (t₁), a known volume of 100% CO₂ was introduced into each pouch, the content was manually agitated and a new 0.5 ml sample was withdrawn and introduced into the G.C. The new response resulted from the increase of the initial concentration of CO₂. The volume of the pouch was determined using equation 1.

Results-Discussion

Equation (1) was developed for the determination of the pouch volume, assuming that $\frac{V_p}{V_p + V_{CO_2}} \cong 1$, or $V_p \gg V_{CO_2}$

where :

$$\frac{V_{CO_2}}{V_p + V_{CO_2}} = \frac{C_2 - C_1}{100} \quad (1)$$

V_{CO_2} = Volume of 100% CO₂ injected into the pouch (ml)

V_p = Volume of pouch (ml)

C_1 = % CO₂ concentration (g/ml) inside pouch before introduction of 100 CO₂

C_2 = % CO₂ concentration (g/ml) inside pouch after » of 100 CO₂

The permeability values were calculated as follows :

At time t₁ the G.C. response is converted to % CO₂ concentration $C_1 \left(\frac{W}{V} \right)$

using the standard curve.

(α_1) = amt. of CO₂ perm. into pouch at time t₁ = $C_1 \times 10^{-2} \times V_p$ or $C_1 = \frac{\alpha_1 100}{V_p}$

The same calculations are carried out for sampling times t₂, t₃,... Next the plot amt. of CO₂ permeated versus time is constructed. Finally the permeability value is calculated as the ratio :

$$\text{Perm. Val.} = \frac{\text{slope of curve (ml/day)}}{\text{Area of pouch} \times \text{P.Pressure difference (m}^2 \cdot \text{atm.)}}$$

Comparison of the method proposed with the «permeability cell» method⁶ was accomplished for three of the film samples provided and results shown in Table I, correlate fairly well between the two methods.

TABLE I : CO₂ permeability values of films# 1004,1019 and 1001 using both the «pouch» method and the «permeability cell» method.

Film N ^o	CO ₂ permeability values (in ml/m ² .24hrs.atm)	
	proposed «pouch» method	«permeability cell» method
1004	6.8	7.7
1019	20.5	22.8
1001	66.8	72.9

Lower Permeability values calculated for the «pouch» method are probably owed to the relatively high permeation rate of the silicon septum to CO₂. Once the pouch is pinched twice or more by the needle the CO₂ content of the pouch decreases during the procedure of sampling.

Results of the CO₂ permeability measurements from twelve different film laminates tested, using the proposed method, are summarized in Table II. Permeability values are expressed in ml/m².24 hrs.atm. Each value is the mean of duplicate measurements.

TABLE II : CO₂ permeability values of various film laminates using the proposed «pouch method»

Film N ^o	laminate composition from inside → out	CO ₂ Permeability value (ml/m ² .24hrs.atm)	
		Mean Rel.	Width
1001	PET/Saran/MDPE	66.8	10.3
1002	PET/double Saran/LDPE	18.8	9.6
1003	PET/Alum. foil/Surlyn/Polyurathane	~0	0
1004	PET/Saran/Epoxy/Saran/Surlyn	6.8	10.3
1019	Polyester/double Saran	20.5	10.7
1020	Polyester/Saran/Surlyn/PE	29.1	8.9
1030	LDPE/PVA/Polyester	~0	0
1032	AC/LDPE	~0	0
2001	HDPE/PET/LDPE	394	12.7
2002	EMA/LDPE/PP/LDPE	1440	13.6
5010	PE/PP/LDPE/EMA (blister package)	14061	15.7
5020	Surlyn/PP/LDPE/EMA (blister package)	13722	15.8

PET = Polyethylene terephthalate

MDPE = Medium density polyethylene

LDPE = Low density polyethylene

HDPE = High density polyethylene

PP = Polypropylene

PVA = Polyvinyl alcohol

AC = Acrylonitrile

In conclusion, it is stated that the method described above can be used interchangeably with the «permeability cell» method, for any film, providing that a pouch can be formed from the plastic film material.

The obvious advantage of the proposed method is that it is inexpensive and it can handle a great number of film samples simultaneously.

Abstract

In recent food and drug packaging applications, a wide variety of plastic films is being used, each one possessing its own specific barrier properties.

The type of films selected for each application will be determined by the nature of the specific product being packaged. Moisture and oxygen sensitive foods and drugs will need a low oxygen and water vapor permeability material to provide increased protection or a longer «shelf life» to the product. In this paper a modification of the «permeability cell» method, for the determination of CO₂ permeation rates in various plastic films is proposed.

Περίληψη

Απλή μέθοδος προσδιορισμού της διαπερατότητας πλαστικών μεμβρανών που χρησιμοποιούνται στη συσκευασία τροφίμων και φαρμάκων

Στις σύγχρονες εφαρμογές της συσκευασίας τροφίμων και φαρμάκων χρησιμοποιείται μεγάλη ποικιλία πλαστικών υλικών συσκευασίας, το καθένα με αυστηρά καθορισμένη τη διαπερατότητά του στα αέρια (O₂, CO₂) και τους υδρατμούς.

Η επιλογή του υλικού που θα χρησιμοποιηθεί στην κάθε περίπτωση εξαρτάται από τη φύση του προϊόντος που θα συσκευαστεί. Τρόφιμα και φάρμακα ευαίσθητα στο οξυγόνο και στους υδρατμούς απαιτούν υλικά πολύ χαμηλής διαπερατότητας για να αυξηθεί κατά το δυνατόν ο «χρόνος ζωής» του προϊόντος.

Στην εργασία αυτή προτείνεται μια σχετικά απλή μέθοδος, «για τη μέτρηση της διαπερατότητας σε CO₂ και O₂ διαφόρων πλαστικών υλικών (films), παραλαγή της ήδη χρησιμοποιούμενης διεθνώς μεθόδου «του κυττάρου διαπερατότητας».

Bibliography

1. Tomkins R.C.: *J. Appl. Bact.* **25**, 290 (1962).
2. Jurin V. and Karel M.: *Food Tech.* **17**, 104 (1963).

3. Brady C.J., O'Connell P.B.H., Smydzuk J. and Wade N.O.: *Austr. J. Biol. Sci.* **23**, 1143 (1970).
4. Hesselman C.W. and Freebairn H.T.: *J. Am. Soc. Hort. Sci.* **98**, 631 (1969).
5. Quazi M.H. and Freebairn H.T.: *Bot. Gaz.* **131**, 5 (1970).
6. Karel M., Issenberg D., Ronsivalli L., and Jurin V.: *Food Tech.* **17**, 91 (1963).
7. Gilbert S.G. and Pegaz D.: *Packaging Engineering* **1**, 66 (1969).
8. Herrero F.M. and Waibel J.: *Verpackungs-Rundschau* **27(3)**, 19 (1976).
9. Linowitzki V.: *Verpackungs-Rundschau* **29(9)**, 65 (1978).
10. Rouiller M., Pottier L., Deymie B.: *Emballages* **48(357)**, 153 (1978).